A Comparative Study of Site-Specific Distribution of Aging-Related Tau Astrogliopathy and Its Risk Factors Between Alzheimer Disease and Cognitive Healthy Brains: The Hisayama Study

八木田, 薫

Journal of Neuropathology and Experimental Neurology

A Comparative Study of Site-Specific Distribution of Aging-Related Tau Astrogliopathy and Its Risk Factors Between Alzheimer Disease and Cognitive Healthy Brains: The Hisayama Study

--Manuscript Draft--

Manuscript Number:	JNEN-21-204R1
Full Title:	A Comparative Study of Site-Specific Distribution of Aging-Related Tau Astrogliopathy and Its Risk Factors Between Alzheimer Disease and Cognitive Healthy Brains: The Hisayama Study
Article Type:	Original Article
Keywords:	Aging-related tau astrogliopathy, Alzheimer disease, Astrocyte, Olfactory nerve, Primary age-related tauopathy.
Corresponding Author:	Hiroyuki Honda, Ph.D., M.D. Graduate School of Medical Sciences, Kyushu University Fukuoka, JAPAN
Corresponding Author Secondary Information:	
Corresponding Author's Institution:	Graduate School of Medical Sciences, Kyushu University
Corresponding Author's Secondary Institution:	
First Author:	Kaoru Yagita, M.D
First Author Secondary Information:	
Order of Authors:	Kaoru Yagita, M.D
	Hiroyuki Honda, M.D, PhD
	Tomoyuki Ohara, M.D, PhD
	Hideomi Hamasaki, PhD
	Sachiko Koyama, B.Sc
	Hideko Noguchi, B.Sc
	Akane Mihara, M.D
	Taro Nakazawa, M.D
	Jun Hata, M.D, Ph.D
	Toshiharu Ninomiya, M.D, PhD
	Toru Iwaki, M.D, PhD
Order of Authors Secondary Information:	
Abstract:	Knowledge of aging-related tau astrogliopathy (ARTAG) in healthy elderly individuals remains incomplete and studies to date have not focused on the olfactory nerve, which is a vulnerable site of various neurodegenerative disease pathologies. We performed a semiquantitative evaluation of ARTAG in 110 autopsies in the Japanese general population (Hisayama study). Our analysis focused on Alzheimer disease (AD) and cognitive healthy cases (HC), including primary age-related tauopathy. Among the various diseased and non-diseased brains, ARTAG was frequently observed in the amygdala. The ARTAG of HC was exclusively limited to the amygdala whereas gray matter ARTAG in AD cases was more prominent in the putamen and middle frontal gyrus than in the amygdala. ARTAG of the olfactory nerve mainly consists of subpial pathology that was milder in the amygdala. A logistic regression analysis revealed that age at death and neurofibrillary tangle Braak stage significantly affected the ARTAG of HC. In AD, age at death and male gender had significant effects on ARTAG. In

	addition, the Thal phase significantly affected the presence of white matter ARTAG. In conclusion, our research revealed differences in the distribution of ARTAG and affected variables across AD and HC individuals.

Cover Sheet

Manuscript number: MS21-204R1

Date sent to LWW: November 10, 2021

Authors: Kaoru Yagita[1], MD, Hiroyuki Honda[1], MD, PhD, Tomoyuki Ohara[2,3], MD, PhD, Hideomi Hamasaki[1], PhD, Sachiko Koyama[1], BSc, Hideko Noguchi[1], BSc, Akane Mihara[2,3], MD, Taro Nakazawa[2,3], MD, Jun Hata[3,4,5], MD, PhD, Toshiharu Ninomiya[3,4], MD, PhD, and Toru Iwaki[1], MD, PhD

Title of Article: **A Comparative Study of Site-Specific Distribution of Aging-Related Tau Astrogliopathy and Its Risk Factors Between Alzheimer Disease and Cognitive Healthy Brains: The Hisayama Study**

Short title: *Progression of ARTAG at AD and PART*

Corresponding Author: Hiroyuki Honda

Address of Corresponding Author: Department of Neuropathology, Graduate School of Medical Sciences, Kyushu University, Fukuoka, Japan, 812-8582

E-mail: honda.hiroyuki.211@m.kyushu-u.ac.jp

Tables: 4

Digital Art: do not remake

Figures: 3
Color Figures: 3

NIH Funding: NA

Open Access: NA

Supplemental Materials: 1 figure + 5 tables

Permissions: NA

Special Instructions: NA

Running head title: Progression of ARTAG at AD and PART

A Comparative Study of Site-Specific Distribution of Aging-Related Tau Astrogliopathy and Its Risk Factors Between Alzheimer Disease and Cognitive Healthy Brains: The Hisayama Study

Kaoru Yagita[1], MD, Hiroyuki Honda[1], MD, PhD, Tomoyuki Ohara[2,3], MD, PhD, Hideomi Hamasaki[1], PhD, Sachiko Koyama[1], BSc, Hideko Noguchi[1], BSc, Akane Mihara[2,3], MD, Taro Nakazawa[2,3], MD, Jun Hata[3,4,5], MD, PhD, Toshiharu Ninomiya[3,4], MD, PhD, and Toru Iwaki[1], MD, PhD

[1] Department of Neuropathology, Graduate School of Medical Sciences, Kyushu University, Fukuoka, Japan;

[2] Department of Neuropsychiatry, Graduate School of Medical Sciences, Kyushu University, Fukuoka, Japan;

[3] Department of Epidemiology and Public Health, Graduate School of Medical Sciences, Kyushu University, Fukuoka, Japan;

[4] Department of Center for Cohort Studies, Graduate School of Medical Sciences, Kyushu University, Fukuoka, Japan;

[5] Department of Medicine and Clinical Science, Graduate School of Medical Sciences, Kyushu University, Fukuoka, Japan.

Send correspondence to: Hiroyuki Honda, Department of Neuropathology, Graduate School of Medical Sciences, Kyushu University, Fukuoka, Japan, 812-8582. E-mail:

honda.hiroyuki.211@m.kyushu-u.ac.jp

This study was supported in part by the Agency for Medical Research and Development (JP20dk0207025).

The authors have no conflicts of interest to declare.

Abstract

Knowledge of aging-related tau astrogliopathy (ARTAG) in healthy elderly individuals remains incomplete and studies to date have not focused on the olfactory nerve, which is a vulnerable site of various neurodegenerative disease pathologies. We performed a semiquantitative evaluation of ARTAG in 110 autopsies in the Japanese general population (Hisayama study). Our analysis focused on Alzheimer disease (AD) and cognitive healthy cases (HC), including primary age-related tauopathy. Among the various diseased and non-diseased brains, ARTAG was frequently observed in the amygdala. The ARTAG of HC was exclusively limited to the amygdala whereas gray matter ARTAG in AD cases was more prominent in the putamen and middle frontal gyrus than in the amygdala. ARTAG of the olfactory nerve mainly consists of subpial pathology that was milder in the amygdala. A logistic regression analysis revealed that age at death and neurofibrillary tangle Braak stage significantly affected the ARTAG of HC. In AD, age at death and male gender had significant effects on ARTAG. In addition, the Thal phase significantly affected the presence of white matter ARTAG. In conclusion, our research revealed differences in the distribution of ARTAG and affected variables across AD and HC individuals.

Key words: Aging-related tau astrogliopathy, Alzheimer disease, Astrocyte, Olfactory nerve, Primary age-related tauopathy.

INTRODUCTION

Nonspecific glial tauopathies have long been recognized in a wide range of neurodegenerative diseases that are different from specific tau astrogliopathies, such as tufted astrocytes in progressive supranuclear palsy (PSP), astrocytic plaques in corticobasal degeneration, ramified astrocytes in Pick disease, and globular astrocytic inclusions in globular glial tauopathy (1, 2). Nonspecific abnormal tau accumulation in astrocytes has also attracted attention in light of the growing body of evidence that astrocytes play a significant role in various central nervous system (CNS) diseases. In abnormal tau gliopathies, 2 morphologically distinct findings have been recognized: thorn-shaped astrocytes (TSA) exhibiting phosphorylated tau accumulation in perinuclear and proximal/distal protrusions, and granular or fuzzy astrocytes (GFA) involving fine punctate changes in the proximal and distal processes. Aging-related tau astrogliopathy (ARTAG) was suggested as a neuropathological term, encompassing a wide spectrum of tau astrogliopathies in 2016 (1).

Systematic neuropathological analysis of ARTAG in 628 brain bank cases disclosed that age at death, male gender, and frontotemporal lobar degeneration tauopathy are associated with ARTAG (3). Another brain bank-based evaluation of GFA revealed an association with primary tauopathies such as PSP and argyrophilic grain disease (AGD). However, a significant association with age at death was not detected in that study (4). The amygdala is considered to be the most frequently affected site of ARTAG but definitive relationships between ARTAG and neuronal tauopathies have not been demonstrated and the mechanisms of ARTAG formation remain unknown. The sequential pattern of ARTAG involvement indicates that tau astrogliopathy is mainly initiated in the amygdala and spreads to other brain regions whereas some gray matter (GM) ARTAG spreads from the striatum to other sites, including the amygdala. This implies that

ARTAG may exhibit discrete behaviors according to specific disease subtype (5).

ARTAG is found not only in numerous CNS diseases but is also found in mentally normal elderly individuals and may be associated with primary age-related tauopathy (PART). As such, it may reflect reduced brain metabolism during aging (1, 4). However, previous studies on ARTAG were performed on brains of patients with CNS diseases collected in brain banks; elderly individuals without cognitive disorders remain to be investigated. The Hisayama study is a prospective cohort study of cerebral/cardiovascular diseases and dementia in general Japanese residents. This study previously revealed trends of dementia prevalence and increasing tauopathy and an association between insulin resistance and Alzheimer disease (AD) (6–8).

We sought to clarify the extent of ARTAG in the general elderly population, including in people without cognitive diseases, based on the consecutive autopsies of the Hisayama study. We then compared site-dependent progression of ARTAG in AD.

Materials and Methods

Subjects

A population-based prospective study (the Hisayama study) was conducted in 1961 in the town of Hisayama, a suburban community adjacent to Fukuoka City, a metropolitan area of Kyushu Island in southern Japan. The population of Hisayama is approximately 8,400 and has been stable for the past 50 years (9, 10). Comprehensive surveys of cognitive impairment in the elderly population of this town have been conducted since 1985. In the present study, we examined a series of 110 autopsies that were performed between November 11, 2017 and March 2, 2020 on residents of Hisayama (mean age at death: 85.2 ± 9.11 years; age range: 61–104 years). A total of 226 residents died during this period; of these, 138 underwent autopsy examination (the autopsy rate was 61.1%). Neuropathological evaluation was not performed in 9 autopsy cases, and 19 brain specimens were not viable for analysis mostly because of olfactory nerve impairment during autopsy. The profiles of the examined cases are summarized in Table 1. This study was approved by the Ethics Committee of the Faculty of Medicine, Kyushu University (#2020-167), and was carried out in accordance with the ethical standards described in the fifth revision of the Declaration of Helsinki, 2000.

Histopathology and Immunohistochemistry

Brains were weighed and fixed with 10% buffered formaldehyde for at least 2 weeks. The brain specimens investigated included the olfactory nerve, middle frontal gyrus, basal ganglia, superior and middle temporal gyri, amygdala, hippocampus, entorhinal cortex, and transentorhinal cortex (at the level of the lateral geniculate body), precentral gyrus, thalamus, inferior parietal lobule, anterior cingulate gyrus, midbrain, pons, and medulla oblongata. Sections were embedded in paraffin and routinely stained with hematoxylin and eosin and Klüver-Barrera staining.

Immunohistochemistry was performed using primary antibodies against phosphorylated tau (AT8, 90206 mouse monoclonal, 1:500; Innogenetics, Ghent, Belgium), amyloid beta (Aβ) (M0872 mouse monoclonal, 1:200; Dako, Glostrup, Denmark), phosphorylated α-synuclein (p-αS) (015-25191 mouse monoclonal, 1:2000; Wako, Osaka, Japan), 3-repeat tau (RD3, 05-803 mouse monoclonal, 1:1000; Upstate Biotechnology, Buffalo, NY), 4-repeat tau (RD4, 05-804 mouse monoclonal, 1:200; Millipore, Burlington, MA), and phosphorylated TAR DNA-binding protein of 43 kDa (p-TDP-43) (TIP-PTD-M01 mouse monoclonal, 1:4000; Cosmo Bio, Tokyo, Japan). The sections were incubated with 0.3% H_2O_2 in methanol for 30 minutes to inactivate the intrinsic peroxidase. We performed pretreatments for antigen retrieval by 60-minute incubation in 90% formic acid when using anti-Aβ antibody, autoclave for 10 minutes in 10 mM sodium citrate buffer at 121°C, using AT8, anti-pαS, and anti-p-TDP-43 antibodies, and 10 mM sodium citrate buffer autoclave after 10-minute incubation with 90% formic acid when using RD3 and RD4. The specimens were incubated overnight at 4°C with primary antibodies. Immunoreaction products were detected by the polymer immunocomplex method using the Envision system (Dako) and visualized using 3, 3′-diaminobenzidine ([DAB]; Dojindo, Kumamoto, Japan). Nuclei were subsequently counterstained with hematoxylin.

Double-labeling immunofluorescence was performed using a combination of AT8 (1:200) and GFAP (Z0334 rabbit polyclonal, 1:500; Dako). Deparaffinized samples were treated with primary antibodies that were blocked with normal goat serum at 4°C overnight, and then reacted with a mixture of fluorophore-labeled secondary antibodies (Alexa Fluor 488 goat anti-mouse and Alexa Fluor 546 goat anti-rabbit, 1:200 each; Thermo Fisher Scientific, Waltham, MA) at room temperature in the dark for one hour. Sections were mounted with ProLong Gold Antifade

Mountant with DAPI (Thermo Fisher Scientific). Images were acquired using a Nikon A1 confocal microscope (Nikon, Tokyo, Japan).

Evaluation of Standard and ARTAG Pathology

Well-experienced neuropathologists assessed standard brain pathological diagnosis, CERAD, Thal phase, and Braak stage of neurofibrillary tangle (NFT). A semiquantitative evaluation of ARTAG pathology was performed by another neuropathologist in a blinded manner with regard to clinical and pathological diagnosis, similar to the previous investigation: 0, absent; 1, occasional and focal; 2, numerous focal or scattered widespread; 3, numerous widespread (1, 3, 11). We identified different types of ARTAGs according to their location: subpial, subependymal, GM, white matter (WM), and perivascular ARTAG, as previously described (1, 3, 11).

ARTAG severity was assessed in specimens including the middle frontal gyrus, basal ganglia, superior/middle temporal gyrus, amygdala, hippocampus/parahippocampal gyrus, inferior parietal lobule, midbrain, pons, medulla oblongata, and ON. Next, we scored each type of ARTAG depending on the affected areas as follows: Subpial ARTAG: all regions excluding the basal ganglia; Subependymal ARTAG: amygdala, hippocampus, and brainstem; GM/WM ARTAG: all regions; Perivascular ARTAG: all regions except the olfactory nerve.

We also assessed other neurodegenerative changes (senile plaques, NFT, Lewy bodies [LBs], and p-TDP-43 neuronal cytoplasmic inclusions [NCIs]) in the amygdala. The severity of senile plaques was assessed by CERAD, and semiquantitative evaluations with respect to the distribution of NFTs and Lewy bodies were performed. Distribution was rated as follows: 0, none/absent; 1, sparse/occasional; 2, moderate; 3, frequent/numerous. We defined a score of 2 or higher CERAD/NFTs/LBs as events. The p-TDP-43 NCIs were evaluated on the basis of their

presence as they showcased relatively low frequency.

Statistical Methods

Values between any 2 groups were assessed by a Mann-Whitney U test, Chi-squared test, and Spearman-rank test. The Steel-Dwass test was used as a multiple comparison test. To investigate whether senescent neuropathological changes are associated with ARTAG severity, binary logistic regression models were used, and the predictor variables included age at death, sex, Thal phase, and Braak stage of NFT. Multiple logistic regression analysis was performed to evaluate the association between ARTAG and other neurodegenerative changes (senile plaques, NFT, Lewy bodies, and p-TDP-43 NCIs) in the amygdala, adjusting for sex and age at death. JMP ver 15.2 (SAS Institute, Cary, NC) was used for all statistical analyses.

RESULTS

Overview of Autopsy Cases

Table 1 summarizes the total of 110 autopsy cases. The average age at death was 85.3 years and clinicopathological profiles included cognitively healthy patients ([HC], 47 cases), AD (41 cases), vascular dementia (VD, 8 cases), dementia with Lewy bodies ([DLB], 5 cases), senile dementia of the neurofibrillary tangle type ([SD-NFT], 4 cases), PSP (3 cases), and AGD (2 cases). In the case of comorbid disease, we sorted the cases according to the most prominent neuropathological changes. Subjects who showed no sign of cognitive disturbance during life were designated as HC. All HC were elderly people (61-102 years old) and presented at least minimal tauopathies, as reported in our previous studies (7). PART cases diagnosed as dementia while alive were classified as SD-NFT. ARTAGs were found in all PSP and AGD cases despite the small number of samples, which is consistent with previous studies (3, 4).

ARTAG Distribution and Morphological Characteristics

Most subpial, subependymal, and perivascular ARTAGs consisted of TSA in focal regions. In the cases burdened with heavy tau glial pathological changes, highly dense glial lesions were sequentially detected through 2 discrete locations, subpial and perivascular, or subependymal and perivascular areas (Fig. 1A-C). In contrast, GM ARTAG was usually identified as GFA and tended to be widely distributed without any signs of focal accumulation (Fig. 1D, E). Small clusters of ARTAG often appear in the vicinity of subpial/perivascular/WM ARTAGs. Many WM ARTAGs were composed of TSA (Fig. 1F), while GFA was recognized in cases of mild tau gliopathy. As previously described, these glial tauopathies consisted of 4 repeat-tau, whereby they did not show any signs of 3 repeat-tau components (1, 3) (Fig. 1G-I).

The amygdala is a common ARTAG hotspot in AD, HC, SD-NFT, VD, and DLB (Fig. 2; Supplemental Fig. 1). In HC, SD-NFT, and VD, all ARTAGs were found exclusively in the amygdala. AD ARTAG was also found to be heavily concentrated in the amygdala, while gray matter tau gliopathy was dispersed across the putamen and the middle frontal gyrus to a lesser degree. The Steel-Dwass test revealed significant differences in GM ARTAG of HC between the amygdala and all other brain regions except the parahippocampal gyrus, while in GM ARTAG of AD, there were no significant differences across the amygdala, putamen, and middle frontal gyrus (Supplementary Tables 1, 2).

DLB cases exhibited an ARTAG distribution pattern similar to that of HC. ARTAG of AGD cases mainly consisted of GM and WM glial tauopathy, which revealed a spreading pattern similar to that of AD. GM and WM tau glial pathology were also dominant in PSP and were strongly observed in the middle frontal gyrus, putamen, superior/middle temporal gyrus, and midbrain, which is the same distributional pattern of tufted astrocytes (Supplementary Fig. 1) (11). All ARTAG subtypes were found in the amygdala. Additionally, we investigated whether ARTAG could be associated with other proteinopathies in the amygdala. The multiple logistic regression analysis, adjusting for sex and age at death with respect to GM/WM ARTAG, showed significant negative effects on senile plaques (Supplementary Table 3). Subpial ARTAG significantly affected the presence of p-TDP-43 NCIs presence (OR: 1.08, 95% COI: 1.01-1.17, p value: 0.009). No subtype of ARTAG showed significant effect on NFTs and LBs.

Pathological Assessments of Astroglial Tauopathy in Olfactory Nerves

Tau astrogliopathy of the olfactory nerves was primarily observed in the subpial regions and was predominantly distributed in proximal regions (Fig. 3A, B). These pathological alterations were

milder than those in the amygdala. Cases of marked glial tauopathy contained white matter lesions along the olfactory nerve fibers (Fig. 3C). However, there was no obvious tau gliopathy in the gray matter, such as the anterior olfactory nucleus (Fig. 3D-F). Additional evaluations included 11 cases (6 AD, 4 HC, and 1 VD) that had severe astrocytic phosphorylated tau lesions of the olfactory nerve. Phosphorylated tau-positive glial lesions manifested mostly as 4-repeat tau, whereas these gliopathies were not composed of 3-repeat tau (Fig. 3G-I). Confocal double immunofluorescence of a combination of AT8 and anti-GFAP antibodies revealed colocalization of phosphorylated tau accumulation in astrocytes (Fig. 3J-L). Thus, tau gliopathies of the olfactory nerve were similar to the cytological changes in ARTAG observed across other regions.

Associations Between ARTAG and Different Variables Across AD and HC Individuals

Spearman rank correlation test for ARTAG severity and different variables revealed that age at death and NFT Braak stage are associated with all the subtypes of ARTAG the entire cohort (Supplementary Table 4). Moreover, all the subtypes were found to be negatively related to brain weight, except for the GM subtype. On the other hand, every subtype of ARTAG in HC correlated with age at death, NFT Braak stage, and CERAD. Subpial/GM/WM/perivascular glial pathology revealed a correlation with the Thal phase. Subpial/WM ARTAG in AD was associated with age at death, and WM glial tauopathy was related to the Thal phase. None of the AD subtypes showed a significant correlation with the NFT Braak stage.

A multiple logistic regression analysis was performed to evaluate the effect of variables (age at death, sex, Thal phase, NFT Braak stage) on ARTAG in the entire cohort (Table 2). As reported in our previous study, age at death significantly affected the presence of every ARTAG subtype. The NFT Braak stage also exhibited significant effects; however, the results were different from

those previous investigations (3, 4). These discrepancies may be due to the difference in the population sample. The present study was of general Japanese residents, and predominantly included AD and HC individuals whereas previous investigations were based on various diseased brain bank subjects. Therefore, we additionally performed a separate logistic regression analysis for the AD and HC groups (Tables 3, 4). The NFT Braak stage had a significant effect on the presence of every subtype of ARTAG in HC. The age at death variable also demonstrated a significant effect on every subtype of ARTAG in HC, except for subependymal glial tauopathy. In the AD group, we could not find any variables showing a significant effect on the existence of subependymal and perivascular ARTAGs. The age at death variable significantly influenced the appearance of all the types of ARTAG, including subpial, gray matter, and white matter ARTAG. Male gender had significant effects on the presence of all types, gray matter, and white matter ARTAG, whereas the Thal phase significantly affected the existence of all types and white matter ARTAGs. Contrary to expectations, the NFT Braak stage showed a significant effect on the lower odds ratio of all types of ARTAG, including the gray matter and white matter ARTAG in AD.

Clinical Characteristics of ARTAG Pathology

We compared the Mini-Mental State Examination (MMSE) scores of subcortical white matter ARTAG-positive (11 cases) and negative (28 cases) AD groups. These 2 groups demonstrated no significant differences in age, sex, brain weight, CERAD, and NFT Braak staging scores, while white matter ARTAG-positive AD exhibited a significantly higher Thal phase (4.91 vs 4.21, $p = 0.027$). This outcome was reconcilable with the result that the Thal phase had a significant effect on the presence of white matter ARTAG. It has been previously reported that a higher density of subcortical white matter ARTAG correlates with poor language function in AD (12). Therefore,

we evaluated the influence of white matter ARTAG on language dysfunction among the AD group in our study. The language associated with the MMSE total score (sum of naming, repeating, 3 step orders, reading and writing) was observed to be low in the white matter positive ARTAG group (7.36 vs 7.67, p value = 0.070). However, the total MMSE scores in both groups were very similar (26.00 vs 26.04, p value = 0.912).

ARTAG was seen in the amygdala of all types of neurodegenerative diseases. We explored medical records to assess whether the severe burden of ARTAG led to a disturbance of the amygdala, thus causing mood/psychotic symptoms. Severe amygdala ARTAG cases were defined as those involving excessive amygdala lesions as compared to numerous focal or scattered widespread ARTAG (score 2). The medical records of AD and HC were retrospectively investigated (Supplementary Table 5). Episodes of mood/psychotic dysfunction, such as irritability, depression, and pica behavior were reported in 5/17 severe amygdala ARTAGs in AD patients, while delusions, depression, and hallucinations were identified in 10/24 AD patients without severe amygdala ARTAG. The prevalence across the 2 groups was not significantly different (p value = 0.422). In terms of HC, 1/13 severe ARTAG cases suffered from depression and 4/34 non-severe cases exhibited mood/psychotic disturbances such as depressed mood, alcohol dependence, and refusal to accept medical care. There was no significant difference between the prevalence of the 2 classifications (p = 0.685).

DISCUSSION

This study revealed features of ARTAG pathology in AD patients and cognitively healthy elderly individuals affected by PART in a community-based clinicopathological cohort study. Most previous studies evaluating ARTAG were performed on diseased cerebrums collected from brain banks; therefore, there is insufficient knowledge about the non-diseased brain of the elderly (3, 4, 11, 12). We evaluated sequential autopsy cases in general Japanese residents and included a large number of patients of 2 representative senile neuropathological states, AD and PART, without dementia (41 and 47 cases, respectively). Thus, this is the first study to describe distinct ARTAG characteristics between AD and HC without bias. The amygdala is a common hotspot of all ARTAG subtypes, and both senile states show a similar correlation with age at death, as previously described (3–5). However, the gray matter was strongly affected in the amygdala, putamen and middle frontal gyrus in AD, while tau gliopathy of HC was more restricted to the amygdala. Our study also revealed that age at death and male sex influenced all types of ARTAG, and only WM ARTAG in AD was related to the Thal phase as confirmed by the previous study findings (3). In contrast, however, this was the first study that revealed the association of distinct factors, i.e. age at death and NFT Braak stage, with ARTAG in HC.

Previous assessments have revealed that the amygdala is a common hotspot of ARTAG in various neurodegenerative brain diseases (3, 4). Kovacs et al reported the sequential distribution pattern of each subtype of ARTAG and identified 2 pathways of gray matter ARTAG. In one, glial lesions start in the amygdala and spread toward other brain areas and in the other, striatal tau astrogliopathies spread to other brain regions (5). In our study, involvement of the gray matter of the putamen was followed by the amygdala in AD; however, HC containing PART exhibited gray matter lesions that were more intense in the amygdala. While the putamen is a

hotspot of tufted astrocytes in PSP (11), GFA was predominant in the putamen of ARTAG in AD, whereas tufted astrocytes were not.

This study revealed that the features associated with the presence of ARTAG differed between AD and PART. Two factors, age at death and NFT Braak stage, were consistently significant across each subtype of ARTAG in PART, while heterogeneous factors such as aging, sex, and Thal phase related to the generation of different subtypes of ARTAG in AD. Interestingly, male gender was found to influence the ARTAG formation in AD, which is consistent with previous findings (3). A study by Arena et al recently assessed the detailed immunophenotypic characteristics of chronic traumatic encephalopathy (CTE) in 14 cases (13). They revealed that astroglial tau pathology in CTE consisted of 4-repeat tau-positive astrogliopathy, which is indistinguishable from the TSA of ARTAG. The association between CTE and sex difference has not been well investigated because female professionals that are involved in contact sports are generally younger and not enough female brains with a history of repetitive head impacts have been donated for study on a regular basis (14). This said, almost all pathologically proven CTE patients have been male while only one patient was female. Therefore, there may be a common underlying pathological mechanism behind these two tauopathies (14, 15).

Our results also demonstrated that white matter ARTAG was associated with the Thal phase, which is also consistent with a previous report (3). Astrocytes surrounding senile plaques manifest a hypertrophic state and rich GFAP expression (16, 17), and Aβ oligomers themselves provoke astrocyte dysfunction of synaptogenic and synaptic protective capacity (18, 19). White matter ARTAG might be affected by neocortical impairment due to senile plaques because tau aggregation in white matter astroglia is distributed along axonal fibers.

The aging and Braak stages were extensively significant for ARTAG formation in the PART. Senescent astrocytes profoundly modify the cerebral microenvironment by increasing GFAP, vimentin, and senescence-associated secretory phenotype factors (20–22). A recent report revealed that insoluble tau species were less toxic to neurons and astrocytes than soluble species; and neural tau transfer to astrocytes prompted astrocytic tau aggregation (23, 24). Moreover, astrocytes physiologically express very low levels of tau. Therefore, they may relate to cerebral environmental alteration of neural tau increment, and aggregated tau in astrocytes of PART might indicate a slow collapse of aging brain homeostasis (23, 25–27). In contrast, however, several heterogeneous factors were associated with the existence of ARTAG in AD, and the pathological mechanisms influenced by tau pathology might include more elements besides Aβ toxicity, blood-brain barrier dysfunction, and chronic inflammation. On the other hand, the results of logistic regression analysis at the entire population level differed from that of previous investigations (3, 4). Discrepancies among the factors associated with ARTAG can be observed between our study and the previous investigations (3, 4), as well as between the foregoing studies (3, 4). This result may be due to the differences in population samples, which suggests that ARTAG formation can be associated with heterogeneous pathological conditions.

To our knowledge, this is the first study to evaluate astroglial tauopathy of the olfactory nerve. Astrocytic tau aggregation of the olfactory nerve was predominantly composed of subpial injuries. Astroglial tauopathies of the olfactory nerve tract were observed in close proximity to subpial tau aggregation in severe cases, where tau astrogliopathy was absent in the anterior olfactory nuclei despite an abundance of NFT and NT. Almost all astrocytic phosphorylated-tau components were 4-repeat tau in immunohistochemical studies, and confocal double

immunofluorescence staining revealed colocalization of phosphorylated-tau and GFAP. These results were consistent with previous research on ARTAG. As such, we assessed the tau astrogliopathies of the olfactory nerve encompassed within ARTAG (1, 3). The olfactory nerve is particular vulnerable to numerous neurodegenerative diseases, such as AD and Parkinson disease (28, 29). Since olfactory dysfunction is a prodromal symptom of various neurodegeneration and the olfactory epithelium is exposed to the external environment, the olfactory nerve could represent an entry site for pathogens (28, 30). The ARTAG of the olfactory nerve was milder than that of the amygdala, and these tau aggregations tended to be distributed over the proximal part of the olfactory nerve. It is well-established that Lewy body pathology propagates from the peripheral olfactory nerve to the CNS, while ARTAG might initiate from the amygdala and subsequently spread to the olfactory nerve (31, 32). In our study, ARTAG was absent in the anterior olfactory nucleus despite the abundance of NFT. Astrocytes have diverse functions and do not contribute to the brain microenvironment consistently (33, 34). Astrocytes play multiple roles in maintaining homeostasis in respective brain areas, which might play a role in the vulnerability of individual cerebral areas. The divergent distribution of ARTAG might be a reflection of various astrocyte reactions to aging alternation and tau toxicity between distinct brain regions.

Many matters remain to be assessed regarding the relationship between ARTAG and clinical aspects. Some previous studies showed that the ARTAG frequency of atypical AD was equal to that of typical AD, or no clinical impact was observed regarding ARTAG (3, 35). Other investigators reported that the densities of subcortical white matter TSAs in AD were associated with language and spatial dysfunction, or that AD cases who were diagnosed with possible progressive primary aphasia frequently contained cortical/subcortical TSA (12, 36). We

categorized patients with AD based on the presence of subcortical white matter ARTAG and compared their total MMSE scores related to language function. White matter ARTAG-positive AD tended to score lower with regard to language function despite having similar total MMSE scores, which is consistent with a previous report (12). Since we had to use brief neuropsychological examinations such as MMSE, we could not detect significant difference between the two. Astrocytes play important roles in myelin homeostasis by secreting regenerative factors, cholesterol metabolism, and myelin turnover (37–40). Disturbances in astrocytes as a result of tau toxicity may impede salient connections required for language.

A reduction in the number and morphological changes of astrocytes in patients with major depressive disorder has previously been reported (41, 42). These investigations suggest that astrocytes play an important role in neuropsychiatric disorders. Our retrospective review of medical records failed to reveal a significant relationship between ARTAG and mood/psychotic symptoms. Systematic quantitative scrutiny of mood/psychotic dysfunction was not part of the Hisayama study, and this research relied on daily medical records. Therefore, further research is needed to elucidate the effect of ARTAG on psychological disorders.

There are certain limitations of this study. Some cases with a severe burden of tauopathy were problematic in assessing whether lesions originated from neurons or glial cells. Our examination included only obvious astrocytic tauopathy. Therefore, this study may have underestimated the burden of ARTAG. We assessed only 5 brain sites of subependymal lesions as all the specimens did not include vicinities of the cerebral ventricle. Therefore, the analysis of ARTAG around the lateral ventricle and third ventricle was insufficient. This research is based on autopsy examinations in a Japanese population sample. Although autopsy rate in the sample was high, not

every deceased patient was examined. Thus, we cannot exclude a selection bias. In addition, different lifestyles and genetic backgrounds may limit the generalizability of our findings to other (in particular, Western) ethnicities. It was also difficult to perform neuropsychological tests at the terminal phase of dementia, and MMSE data were acquired at the early time of dementia onset. Furthermore, it was difficult to verify the presence of ARTAG is associated with cognitive impairment.

In conclusion, we investigated ARTAG in residents of a Japanese community. The amygdala represents a common hotspot of ARTAG in 2 alternative states of senescence, PART without dementia and AD. However, gray matter ARTAG was prominent in the putamen and middle frontal gyrus in AD following glial tauopathy in the amygdala. A multiple logistic regression analysis revealed that age at death and NFT Braak staging had a significant effect on the existence of ARTAG in HC, while male sex was found to have a significant effect on gray/white matter ARTAG. Moreover, the Thal phase significantly affected white matter ARTAG in AD. These results demonstrated the heterogeneous and complex pathomechanisms that were associated with ARTAG formation in the context of AD and HC.

ACKNOWLEDGMENTS

The authors thank the members of the Hisayama Research Institute for Lifestyle Diseases for their technical assistance. We would like to thank Editage (www.editage.com) for English language editing.

REFERENCES

1. Kovacs GG, Ferrer I, Grinberg LT, et al. Aging-related tau astrogliopathy (ARTAG): harmonized evaluation strategy. Acta Neuropathol 2016;131:87–102
2. Ikeda K, Akiyama H, Arai T, et al. Glial tau pathology in neurodegenerative diseases: Their nature and comparison with neuronal tangles. Neurobiol Aging 1998;19:S85-S91
3. Kovacs GG, Robinson JL, Xie SX, et al. Evaluating the patterns of aging-related tau astrogliopathy unravels novel insights into brain aging and neurodegenerative diseases. J Neuropathol Exp Neurol 2017;76:270–88
4. Miki T, Yokota O, Haraguchi T, et al. Factors associated with development and distribution of granular/fuzzy astrocytes in neurodegenerative diseases. Brain Pathol 2020;30:811–30
5. Kovacs GG, Xie SX, Robinson JL, et al. Sequential stages and distribution patterns of aging-related tau astrogliopathy (ARTAG) in the human brain. Acta Neuropathol Commun 2018;6:50
6. Honda H, Sasaki K, Hamasaki H, et al. Trends in autopsy-verified dementia prevalence over 29 years of the Hisayama study Neuropathology 2016;36:383–7
7. Hamasaki H, Honda H, Okamoto T, et al. Recent Increases in Hippocampal Tau Pathology in the Aging Japanese Population: The Hisayama Study. J Alzheimers Dis 2017;55:613–24
8. Matsuzaki T, Sasaki K, Tanizaki Y, et al. Insulin resistance is associated with the pathology of Alzheimer disease: the Hisayama study. Neurology 2010;75:764–70
9. Kubo M, Hata J, Doi Y, et al. Secular Trends in the Incidence of and Risk Factors for Ischemic Stroke and Its Subtypes in Japanese Population. Circulation 2008;118:2672–8
10. Izumaru K, Hata J, Nakano T, et al. Reduced Estimated GFR and Cardiac Remodeling: A

Population-Based Autopsy Study. Am J Kidney Dis 2019;74:373–81

11. Kovacs GG, Lukic MJ, Irwin DJ, et al. Distribution patterns of tau pathology in progressive supranuclear palsy. Acta Neuropathol 2020;140:99–119

12. Resende EDPF, Nolan AL, Petersen C, et al. Language and spatial dysfunction in Alzheimer disease with white matter thorn-shaped astrocytes. Neurology 2020;94:E1353–64

13. Arena JD, Smith DH, Lee EB, et al. Tau immunophenotypes in chronic traumatic encephalopathy recapitulate those of ageing and Alzheimer's disease. Brain 2020;143:1572–87

14. Phelps A, Mez J, Stern RA, et al. Risk factors for chronic traumatic encephalopathy: A proposed framework. Semin Neurol 2020;40:439–49

15. Roberts GW, Whitwell HL, Acland PR, et al. Dementia in a punch-drunk wife. Lancet 1990;335:918–9

16. Heneka MT, Carson MJ, Khoury J El, et al. Neuroinflammation in Alzheimer's disease. Lancet Neurology 2015;14:388-405

17. Olabarria M, Noristani HN, Verkhratsky A, et al. Concomitant astroglial atrophy and astrogliosis in a triple transgenic animal model of Alzheimer's disease. Glia 2010;58:831–8

18. Diniz LP, Tortelli V, Matias I, et al. Astrocyte transforming growth factor beta 1 protects synapses against Aβ oligomers in Alzheimer's disease model. J Neurosci 2017;37:6797–809

19. Matias I, Morgado J, Gomes FCA. Astrocyte Heterogeneity: Impact to Brain Aging and Disease. Front Aging Neurosci 2019;11:59

20. Clarke LE, Liddelow SA, Chakraborty C, et al. Normal aging induces A1-like astrocyte

reactivity. Proc Natl Acad Sci U S A 2018;115:E1896–905

21. Mombach JCM, Vendrusculo B, Bugs CA. A model for p38MAPK-induced astrocyte senescence. PLoS One 2015;10: e0125217

22. Porchet R, Probst A, Bouras C, et al. Analysis of gial acidic fibrillary protein in the human entorhinal cortex during aging and in Alzheimer's disease. Proteomics 2003;3:1476-85

23. Maté De Gérando A, D'Orange M, Augustin E, et al. Neuronal tau species transfer to astrocytes and induce their loss according to tau aggregation state. Brain 2021;144:1167–82

24. D'Orange M, Aurégan G, Cheramy D, et al. Potentiating tangle formation reduces acute toxicity of soluble tau species in the rat. Brain 2018;141:535–49

25. Asai H, Ikezu S, Tsunoda S, et al. Depletion of microglia and inhibition of exosome synthesis halt tau propagation. Nat Neurosci 2015;18:1584–93

26. Kahlson MA, Colodner KJ. Glial tau pathology in tauopathies: Functional consequences. J Exp Neurosci 2016 PMID: 26884683

27. Chiarini A, Armato U, Gardenal E, et al. Amyloid β-exposed human astrocytes overproduce phospho-tau and overrelease it within exosomes, effects suppressed by calcilytic NPS 2143-Further implications for Alzheimer's therapy. Front Neurosci 2017;11:217

28. Rey NL, Wesson DW, Brundin P. The olfactory bulb as the entry site for prion-like propagation in neurodegenerative diseases. Neurobiol Dis 2018;109:226–48

29. Ubeda-Bañon I, Saiz-Sanchez D, Flores-Cuadrado A, et al. The human olfactory system in two proteinopathies: Alzheimer's and Parkinson's diseases. Transl Neurodegener. 2020;9:22

30. Dando SJ, Mackay-Sim A, Norton R, et al. Pathogens penetrating the central nervous system: Infection pathways and the cellular and molecular mechanisms of invasion. Clin

Microbiol Rev 2014;27:691–726

31. Braak H, Ghebremedhin E, Rüb U,et al. Stages in the development of Parkinson's disease-related pathology. Cell Tissue Res 2004;318:121-34

32. Braak H, Del Tredici K, Rüb U, et al. Staging of brain pathology related to sporadic Parkinson's disease. Neurobiol Aging 2003;24:197–211

33. Chai H, Diaz-Castro B, Shigetomi E, et al. Neural Circuit-Specialized Astrocytes: Transcriptomic, Proteomic, Morphological, and Functional Evidence. Neuron 2017;95:531-549.

34. Rasmussen R, Samson AJ. Astrocytes: Tailored to Support the Demand of Neural Circuits? Cell Syst 2017;5:165-7

35. Nolan A, De Paula Franca Resende E, Petersen C, et al. Astrocytic tau deposition is frequent in typical and atypical Alzheimer disease presentations. J Neuropathol Exp Neurol 2019;78:1112–23

36. Munoz DG, Woulfe J, Kertesz A. Argyrophilic thorny astrocyte clusters in association with Alzheimer's disease pathology in possible primary progressive aphasia. Acta Neuropathol 2007;114:347–57

37. Berghoff SA, Gerndt N, Winchenbach J, et al. Dietary cholesterol promotes repair of demyelinated lesions in the adult brain. Nat Commun 2017;8:1–15

38. Albrecht PJ, Murtie JC, Ness JK, et al. Astrocytes produce CNTF during the remyelination phase of viral-induced spinal cord demyelination to stimulate FGF-2 production. Neurobiol Dis 2003;13:89–101

39. Dutta DJ, Woo DH, Lee PR, et al. Regulation of myelin structure and conduction velocity by perinodal astrocytes. Proc Natl Acad Sci U S A 2018;115:11832–7

40. Varela-Echevarría A, Vargas-Barroso V, Lozano-Flores C, et al. Is there evidence for

myelin modeling by astrocytes in the normal adult brain? Front Neuroanat 2017;11:75

41. Rajkowska G, Hughes J, Stockmeier CA, et al. Coverage of blood vessels by astrocytic endfeet is reduced in major depressive disorder. Biol Psychiatry 2013;73:613–21

42. Cotter D, Mackay D, Chana G, et al. Reduced neuronal size and glial cell density in area 9 of the dorsolateral prefrontal cortex in subjects with major depressive disorder. Cereb Cortex 2002;12:386–94

Figure legends

Figure 1. Representative histology of ARTAG. (**A-C**) Subependymal and perivascular ARTAG in the amygdala of a cognitive healthy PART subject. Immunohistochemical analysis of phosphorylated tau (AT8) revealed thorn-shaped astrocytes (TSA) with dense tau deposits in subependymal (**B**) and perivascular areas (**C**). (**D-F**) Amygdala of the same case also exhibited gray matter and white matter ARTAG. Gray matter ARTAG mostly consisted of granular/fuzzy astrocytes (**E**) while most of white matter ARTAG consisted of TSA (**F**). Representative subpial ARTAG in a subject with Alzheimer disease demonstrated their phosphorylated tau components (**G**: AT8), which comprised 4-repeat tau (**I**: RD4), but not 3-repeat tau (**H**: RD3).

Figure 2. Mosaic plot of each ARTAG distribution subtype with respect to Alzheimer disease (AD) and cognitively healthy cases (HC). Asterisks denotes the sites exhibiting mild ARTAG with significant difference to that of amygdala by Steel-Dwass test ($p < 0.05$). MFG, middle frontal gyrus; STG/MTG, superior temporal gyrus and middle temporal gyrus; PVC, primary visual cortex; Hippo, hippocampus; Parahippo, parahippocampal gyrus; Amyg, amygdala; OlfN, olfactory nerve; Put, putamen; GP, globus pallidus; MB, midbrain; MO, medulla oblongata.

Figure 3. Representative images of astroglial tauopathy of olfactory nerves. A-C: Immunohistochemical study of phosphorylated tau (AT8) revealed thorn-shaped astrocytes (TSA) in subpial regions of olfactory nerves (**A, B**); fewer white matter TSA were observed in the vicinity (**A, C**). (**D-F**) Anterior olfactory nucleus frequently manifested neurofibrillary tangles; however, no obvious glial tauopathy was observed. **G-I**: The tau astrogliopathy of olfactory nerves is composed of 4-repeat tau (**I**: RD4), but not 3-repeat tau (**H**: RD3), similar to ARTAG in other brain sites. (**J-L**) Confocal images of the subpial region of the olfactory nerve

demonstrate that most of the AT8-positive structures (represented in red) were localized in association with the GFAP-positive cellular components (represented in green).

Running head title: Progression of ARTAG at AD and PART

A Comparative Study of Site-Specific Distribution of Aging-Related Tau Astrogliopathy and Its Risk Factors Between Alzheimer Disease and Cognitive Healthy Brains: The Hisayama Study

Kaoru Yagita[1], MD, Hiroyuki Honda[1], MD, PhD, Tomoyuki Ohara[2,3], MD, PhD, Hideomi Hamasaki[1], PhD, Sachiko Koyama[1], BSc, Hideko Noguchi[1], BSc, Akane Mihara[2,3], MD, Taro Nakazawa[2,3], MD, Jun Hata[3,4,5], MD, PhD, Toshiharu Ninomiya[3,4], MD, PhD, and Toru Iwaki[1], MD, PhD

[1] Department of Neuropathology, Graduate School of Medical Sciences, Kyushu University, Fukuoka, Japan;

[2] Department of Neuropsychiatry, Graduate School of Medical Sciences, Kyushu University, Fukuoka, Japan;

[3] Department of Epidemiology and Public Health, Graduate School of Medical Sciences, Kyushu University, Fukuoka, Japan;

[4] Department of Center for Cohort Studies, Graduate School of Medical Sciences, Kyushu University, Fukuoka, Japan;

[5] Department of Medicine and Clinical Science, Graduate School of Medical Sciences, Kyushu University, Fukuoka, Japan.

Send correspondence to: Hiroyuki Honda, Department of Neuropathology, Graduate School of Medical Sciences, Kyushu University, Fukuoka, Japan, 812-8582. E-mail:

honda.hiroyuki.211@m.kyushu-u.ac.jp

This study was supported in part by the Agency for Medical Research and Development (JP20dk0207025).

The authors have no conflicts of interest to declare.

Abstract

Knowledge of aging-related tau astrogliopathy (ARTAG) in healthy elderly individuals remains incomplete and studies to date have not focused on the olfactory nerve, which is a vulnerable site of various neurodegenerative disease pathologies. We performed a semiquantitative evaluation of ARTAG in 110 autopsies in the Japanese general population (Hisayama study). Our analysis focused on Alzheimer disease (AD) and cognitive healthy cases (HC), including primary age-related tauopathy. Among the various diseased and non-diseased brains, ARTAG was frequently observed in the amygdala. The ARTAG of HC was exclusively limited to the amygdala whereas gray matter ARTAG in AD cases was more prominent in the putamen and middle frontal gyrus than in the amygdala. ARTAG of the olfactory nerve mainly consists of subpial pathology that was milder in the amygdala. A logistic regression analysis revealed that age at death and neurofibrillary tangle Braak stage significantly affected the ARTAG of HC. In AD, age at death and male gender had significant effects on ARTAG. In addition, the Thal phase significantly affected the presence of white matter ARTAG. In conclusion, our research revealed differences in the distribution of ARTAG and affected variables across AD and HC individuals.

Key words: Aging-related tau astrogliopathy, Alzheimer disease, Astrocyte, Olfactory nerve, Primary age-related tauopathy.

INTRODUCTION

Nonspecific glial tauopathies have long been recognized in a wide range of neurodegenerative diseases that are different from specific tau astrogliopathies, such as tufted astrocytes in progressive supranuclear palsy (PSP), astrocytic plaques in corticobasal degeneration, ramified astrocytes in Pick disease, and globular astrocytic inclusions in globular glial tauopathy (1, 2). Nonspecific abnormal tau accumulation in astrocytes has also attracted attention in light of the growing body of evidence that astrocytes play a significant role in various central nervous system (CNS) diseases. In abnormal tau gliopathies, 2 morphologically distinct findings have been recognized: thorn-shaped astrocytes (TSA) exhibiting phosphorylated tau accumulation in perinuclear and proximal/distal protrusions, and granular or fuzzy astrocytes (GFA) involving fine punctate changes in the proximal and distal processes. Aging-related tau astrogliopathy (ARTAG) was suggested as a neuropathological term, encompassing a wide spectrum of tau astrogliopathies in 2016 (1).

Systematic neuropathological analysis of ARTAG in 628 brain bank cases disclosed that age at death, male gender, and frontotemporal lobar degeneration tauopathy are associated with ARTAG (3). Another brain bank-based evaluation of GFA revealed an association with primary tauopathies such as PSP and argyrophilic grain disease (AGD). However, a significant association with age at death was not detected in that study (4). The amygdala is considered to be the most frequently affected site of ARTAG but definitive relationships between ARTAG and neuronal tauopathies have not been demonstrated and the mechanisms of ARTAG formation remain unknown. The sequential pattern of ARTAG involvement indicates that tau astrogliopathy is mainly initiated in the amygdala and spreads to other brain regions whereas some gray matter (GM) ARTAG spreads from the striatum to other sites, including the amygdala. This implies that

ARTAG may exhibit discrete behaviors according to specific disease subtype (5).

ARTAG is found not only in numerous CNS diseases but is also found in mentally normal elderly individuals and may be associated with primary age-related tauopathy (PART). As such, it may reflect reduced brain metabolism during aging (1, 4). However, previous studies on ARTAG were performed on brains of patients with CNS diseases collected in brain banks; elderly individuals without cognitive disorders remain to be investigated. The Hisayama study is a prospective cohort study of cerebral/cardiovascular diseases and dementia in general Japanese residents. This study previously revealed trends of dementia prevalence and increasing tauopathy and an association between insulin resistance and Alzheimer disease (AD) (6–8).

We sought to clarify the extent of ARTAG in the general elderly population, including in people without cognitive diseases, based on the consecutive autopsies of the Hisayama study. We then compared site-dependent progression of ARTAG in AD.

Materials and Methods

Subjects

A population-based prospective study (the Hisayama study) was conducted in 1961 in the town of Hisayama, a suburban community adjacent to Fukuoka City, a metropolitan area of Kyushu Island in southern Japan. The population of Hisayama is approximately 8,400 and has been stable for the past 50 years (9, 10). Comprehensive surveys of cognitive impairment in the elderly population of this town have been conducted since 1985. In the present study, we examined a series of 110 autopsies that were performed between November 11, 2017 and March 2, 2020 on residents of Hisayama (mean age at death: 85.2 ± 9.11 years; age range: 61–104 years). A total of 226 residents died during this period; of these, 138 underwent autopsy examination (the autopsy rate was 61.1%). Neuropathological evaluation was not performed in 9 autopsy cases, and 19 brain specimens were not viable for analysis mostly because of olfactory nerve impairment during autopsy. The profiles of the examined cases are summarized in Table 1. This study was approved by the Ethics Committee of the Faculty of Medicine, Kyushu University (#2020-167), and was carried out in accordance with the ethical standards described in the fifth revision of the Declaration of Helsinki, 2000.

Histopathology and Immunohistochemistry

Brains were weighed and fixed with 10% buffered formaldehyde for at least 2 weeks. The brain specimens investigated included the olfactory nerve, middle frontal gyrus, basal ganglia, superior and middle temporal gyri, amygdala, hippocampus, entorhinal cortex, and transentorhinal cortex (at the level of the lateral geniculate body), precentral gyrus, thalamus, inferior parietal lobule, anterior cingulate gyrus, midbrain, pons, and medulla oblongata. Sections were embedded in paraffin and routinely stained with hematoxylin and eosin and Klüver-Barrera staining.

Immunohistochemistry was performed using primary antibodies against phosphorylated tau (AT8, 90206 mouse monoclonal, 1:500; Innogenetics, Ghent, Belgium), amyloid beta (Aβ) (M0872 mouse monoclonal, 1:200; Dako, Glostrup, Denmark), phosphorylated α-synuclein (p-αS) (015-25191 mouse monoclonal, 1:2000; Wako, Osaka, Japan), 3-repeat tau (RD3, 05-803 mouse monoclonal, 1:1000; Upstate Biotechnology, Buffalo, NY), 4-repeat tau (RD4, 05-804 mouse monoclonal, 1:200; Millipore, Burlington, MA), and phosphorylated TAR DNA-binding protein of 43 kDa (p-TDP-43) (TIP-PTD-M01 mouse monoclonal, 1:4000; Cosmo Bio, Tokyo, Japan). The sections were incubated with 0.3% H_2O_2 in methanol for 30 minutes to inactivate the intrinsic peroxidase. We performed pretreatments for antigen retrieval by 60-minute incubation in 90% formic acid when using anti-Aβ antibody, autoclave for 10 minutes in 10 mM sodium citrate buffer at 121°C, using AT8, anti-pαS, and anti-p-TDP-43 antibodies, and 10 mM sodium citrate buffer autoclave after 10-minute incubation with 90% formic acid when using RD3 and RD4. The specimens were incubated overnight at 4°C with primary antibodies. Immunoreaction products were detected by the polymer immunocomplex method using the Envision system (Dako) and visualized using 3, 3′-diaminobenzidine ([DAB]; Dojindo, Kumamoto, Japan). Nuclei were subsequently counterstained with hematoxylin.

Double-labeling immunofluorescence was performed using a combination of AT8 (1:200) and GFAP (Z0334 rabbit polyclonal, 1:500; Dako). Deparaffinized samples were treated with primary antibodies that were blocked with normal goat serum at 4°C overnight, and then reacted with a mixture of fluorophore-labeled secondary antibodies (Alexa Fluor 488 goat anti-mouse and Alexa Fluor 546 goat anti-rabbit, 1:200 each; Thermo Fisher Scientific, Waltham, MA) at room temperature in the dark for one hour. Sections were mounted with ProLong Gold Antifade

Mountant with DAPI (Thermo Fisher Scientific). Images were acquired using a Nikon A1 confocal microscope (Nikon, Tokyo, Japan).

Evaluation of Standard and ARTAG Pathology

Well-experienced neuropathologists assessed standard brain pathological diagnosis, CERAD, Thal phase, and Braak stage of neurofibrillary tangle (NFT). A semiquantitative evaluation of ARTAG pathology was performed by another neuropathologist in a blinded manner with regard to clinical and pathological diagnosis, similar to the previous investigation: 0, absent; 1, occasional and focal; 2, numerous focal or scattered widespread; 3, numerous widespread (1, 3, 11). We identified different types of ARTAGs according to their location: subpial, subependymal, GM, white matter (WM), and perivascular ARTAG, as previously described (1, 3, 11).

ARTAG severity was assessed in specimens including the middle frontal gyrus, basal ganglia, superior/middle temporal gyrus, amygdala, hippocampus/parahippocampal gyrus, inferior parietal lobule, midbrain, pons, medulla oblongata, and ON. Next, we scored each type of ARTAG depending on the affected areas as follows: Subpial ARTAG: all regions excluding the basal ganglia; Subependymal ARTAG: amygdala, hippocampus, and brainstem; GM/WM ARTAG: all regions; Perivascular ARTAG: all regions except the olfactory nerve.

We also assessed other neurodegenerative changes (senile plaques, NFT, Lewy bodies [LBs], and p-TDP-43 neuronal cytoplasmic inclusions [NCIs]) in the amygdala. The severity of senile plaques was assessed by CERAD, and semiquantitative evaluations with respect to the distribution of NFTs and Lewy bodies were performed. Distribution was rated as follows: 0, none/absent; 1, sparse/occasional; 2, moderate; 3, frequent/numerous. We defined a score of 2 or higher CERAD/NFTs/LBs as events. The p-TDP-43 NCIs were evaluated on the basis of their

presence as they showcased relatively low frequency.

Statistical Methods

Values between any 2 groups were assessed by a Mann-Whitney U test, Chi-squared test, and Spearman-rank test. The Steel-Dwass test was used as a multiple comparison test. To investigate whether senescent neuropathological changes are associated with ARTAG severity, binary logistic regression models were used, and the predictor variables included age at death, sex, Thal phase, and Braak stage of NFT. Multiple logistic regression analysis was performed to evaluate the association between ARTAG and other neurodegenerative changes (senile plaques, NFT, Lewy bodies, and p-TDP-43 NCIs) in the amygdala, adjusting for sex and age at death. JMP ver 15.2 (SAS Institute, Cary, NC) was used for all statistical analyses.

RESULTS

Overview of Autopsy Cases

Table 1 summarizes the total of 110 autopsy cases. The average age at death was 85.3 years and clinicopathological profiles included cognitively healthy patients ([HC], 47 cases), AD (41 cases), vascular dementia (VD, 8 cases), dementia with Lewy bodies ([DLB], 5 cases), senile dementia of the neurofibrillary tangle type ([SD-NFT], 4 cases), PSP (3 cases), and AGD (2 cases). In the case of comorbid disease, we sorted the cases according to the most prominent neuropathological changes. Subjects who showed no sign of cognitive disturbance during life were designated as HC. All HC were elderly people (61-102 years old) and presented at least minimal tauopathies, as reported in our previous studies (7). PART cases diagnosed as dementia while alive were classified as SD-NFT. ARTAGs were found in all PSP and AGD cases despite the small number of samples, which is consistent with previous studies (3, 4).

ARTAG Distribution and Morphological Characteristics

Most subpial, subependymal, and perivascular ARTAGs consisted of TSA in focal regions. In the cases burdened with heavy tau glial pathological changes, highly dense glial lesions were sequentially detected through 2 discrete locations, subpial and perivascular, or subependymal and perivascular areas (Fig. 1A-C). In contrast, GM ARTAG was usually identified as GFA and tended to be widely distributed without any signs of focal accumulation (Fig. 1D, E). Small clusters of ARTAG often appear in the vicinity of subpial/perivascular/WM ARTAGs. Many WM ARTAGs were composed of TSA (Fig. 1F), while GFA was recognized in cases of mild tau gliopathy. As previously described, these glial tauopathies consisted of 4 repeat-tau, whereby they did not show any signs of 3 repeat-tau components (1, 3) (Fig. 1G-I).

The amygdala is a common ARTAG hotspot in AD, HC, SD-NFT, VD, and DLB (Fig. 2; Supplemental Fig. 1). In HC, SD-NFT, and VD, all ARTAGs were found exclusively in the amygdala. AD ARTAG was also found to be heavily concentrated in the amygdala, while gray matter tau gliopathy was dispersed across the putamen and the middle frontal gyrus to a lesser degree. The Steel-Dwass test revealed significant differences in GM ARTAG of HC between the amygdala and all other brain regions except the parahippocampal gyrus, while in GM ARTAG of AD, there were no significant differences across the amygdala, putamen, and middle frontal gyrus (Supplementary Tables 1, 2).

DLB cases exhibited an ARTAG distribution pattern similar to that of HC. ARTAG of AGD cases mainly consisted of GM and WM glial tauopathy, which revealed a spreading pattern similar to that of AD. GM and WM tau glial pathology were also dominant in PSP and were strongly observed in the middle frontal gyrus, putamen, superior/middle temporal gyrus, and midbrain, which is the same distributional pattern of tufted astrocytes (Supplementary Fig. 1) (11). All ARTAG subtypes were found in the amygdala. Additionally, we investigated whether ARTAG could be associated with other proteinopathies in the amygdala. The multiple logistic regression analysis, adjusting for sex and age at death with respect to GM/WM ARTAG, showed significant negative effects on senile plaques (Supplementary Table 3). Subpial ARTAG significantly affected the presence of p-TDP-43 NCIs presence (OR: 1.08, 95% COI: 1.01-1.17, p value: 0.009). No subtype of ARTAG showed significant effect on NFTs and LBs.

Pathological Assessments of Astroglial Tauopathy in Olfactory Nerves

Tau astrogliopathy of the olfactory nerves was primarily observed in the subpial regions and was predominantly distributed in proximal regions (Fig. 3A, B). These pathological alterations were

milder than those in the amygdala. Cases of marked glial tauopathy contained white matter lesions along the olfactory nerve fibers (Fig. 3C). However, there was no obvious tau gliopathy in the gray matter, such as the anterior olfactory nucleus (Fig. 3D-F). Additional evaluations included 11 cases (6 AD, 4 HC, and 1 VD) that had severe astrocytic phosphorylated tau lesions of the olfactory nerve. Phosphorylated tau-positive glial lesions manifested mostly as 4-repeat tau, whereas these gliopathies were not composed of 3-repeat tau (Fig. 3G-I). Confocal double immunofluorescence of a combination of AT8 and anti-GFAP antibodies revealed colocalization of phosphorylated tau accumulation in astrocytes (Fig. 3J-L). Thus, tau gliopathies of the olfactory nerve were similar to the cytological changes in ARTAG observed across other regions.

Associations Between ARTAG and Different Variables Across AD and HC Individuals

Spearman rank correlation test for ARTAG severity and different variables revealed that age at death and NFT Braak stage are associated with all the subtypes of ARTAG the entire cohort (Supplementary Table 4). Moreover, all the subtypes were found to be negatively related to brain weight, except for the GM subtype. On the other hand, every subtype of ARTAG in HC correlated with age at death, NFT Braak stage, and CERAD. Subpial/GM/WM/perivascular glial pathology revealed a correlation with the Thal phase. Subpial/WM ARTAG in AD was associated with age at death, and WM glial tauopathy was related to the Thal phase. None of the AD subtypes showed a significant correlation with the NFT Braak stage.

A multiple logistic regression analysis was performed to evaluate the effect of variables (age at death, sex, Thal phase, NFT Braak stage) on ARTAG in the entire cohort (Table 2). As reported in our previous study, age at death significantly affected the presence of every ARTAG subtype. The NFT Braak stage also exhibited significant effects; however, the results were different from

those previous investigations (3, 4). These discrepancies may be due to the difference in the population sample. The present study was of general Japanese residents, and predominantly included AD and HC individuals whereas previous investigations were based on various diseased brain bank subjects. Therefore, we additionally performed a separate logistic regression analysis for the AD and HC groups (Tables 3, 4). The NFT Braak stage had a significant effect on the presence of every subtype of ARTAG in HC. The age at death variable also demonstrated a significant effect on every subtype of ARTAG in HC, except for subependymal glial tauopathy. In the AD group, we could not find any variables showing a significant effect on the existence of subependymal and perivascular ARTAGs. The age at death variable significantly influenced the appearance of all the types of ARTAG, including subpial, gray matter, and white matter ARTAG. Male gender had significant effects on the presence of all types, gray matter, and white matter ARTAG, whereas the Thal phase significantly affected the existence of all types and white matter ARTAGs. Contrary to expectations, the NFT Braak stage showed a significant effect on the lower odds ratio of all types of ARTAG, including the gray matter and white matter ARTAG in AD.

Clinical Characteristics of ARTAG Pathology

We compared the Mini-Mental State Examination (MMSE) scores of subcortical white matter ARTAG-positive (11 cases) and negative (28 cases) AD groups. These 2 groups demonstrated no significant differences in age, sex, brain weight, CERAD, and NFT Braak staging scores, while white matter ARTAG-positive AD exhibited a significantly higher Thal phase (4.91 vs 4.21, $p = 0.027$). This outcome was reconcilable with the result that the Thal phase had a significant effect on the presence of white matter ARTAG. It has been previously reported that a higher density of subcortical white matter ARTAG correlates with poor language function in AD (12). Therefore,

we evaluated the influence of white matter ARTAG on language dysfunction among the AD group in our study. The language associated with the MMSE total score (sum of naming, repeating, 3 step orders, reading and writing) was observed to be low in the white matter positive ARTAG group (7.36 vs 7.67, p value = 0.070). However, the total MMSE scores in both groups were very similar (26.00 vs 26.04, p value = 0.912).

ARTAG was seen in the amygdala of all types of neurodegenerative diseases. We explored medical records to assess whether the severe burden of ARTAG led to a disturbance of the amygdala, thus causing mood/psychotic symptoms. Severe amygdala ARTAG cases were defined as those involving excessive amygdala lesions as compared to numerous focal or scattered widespread ARTAG (score 2). The medical records of AD and HC were retrospectively investigated (Supplementary Table 5). Episodes of mood/psychotic dysfunction, such as irritability, depression, and pica behavior were reported in 5/17 severe amygdala ARTAGs in AD patients, while delusions, depression, and hallucinations were identified in 10/24 AD patients without severe amygdala ARTAG. The prevalence across the 2 groups was not significantly different (p value = 0.422). In terms of HC, 1/13 severe ARTAG cases suffered from depression and 4/34 non-severe cases exhibited mood/psychotic disturbances such as depressed mood, alcohol dependence, and refusal to accept medical care. There was no significant difference between the prevalence of the 2 classifications (p = 0.685).

DISCUSSION

This study revealed features of ARTAG pathology in AD patients and cognitively healthy elderly individuals affected by PART in a community-based clinicopathological cohort study. Most previous studies evaluating ARTAG were performed on diseased cerebrums collected from brain banks; therefore, there is insufficient knowledge about the non-diseased brain of the elderly (3, 4, 11, 12). We evaluated sequential autopsy cases in general Japanese residents and included a large number of patients of 2 representative senile neuropathological states, AD and PART, without dementia (41 and 47 cases, respectively). Thus, this is the first study to describe distinct ARTAG characteristics between AD and HC without bias. The amygdala is a common hotspot of all ARTAG subtypes, and both senile states show a similar correlation with age at death, as previously described (3–5). However, the gray matter was strongly affected in the amygdala, putamen and middle frontal gyrus in AD, while tau gliopathy of HC was more restricted to the amygdala. Our study also revealed that age at death and male sex influenced all types of ARTAG, and only WM ARTAG in AD was related to the Thal phase as confirmed by the previous study findings (3). In contrast, however, this was the first study that revealed the association of distinct factors, i.e. age at death and NFT Braak stage, with ARTAG in HC.

Previous assessments have revealed that the amygdala is a common hotspot of ARTAG in various neurodegenerative brain diseases (3, 4). Kovacs et al reported the sequential distribution pattern of each subtype of ARTAG and identified 2 pathways of gray matter ARTAG. In one, glial lesions start in the amygdala and spread toward other brain areas and in the other, striatal tau astrogliopathies spread to other brain regions (5). In our study, involvement of the gray matter of the putamen was followed by the amygdala in AD; however, HC containing PART exhibited gray matter lesions that were more intense in the amygdala. While the putamen is a

hotspot of tufted astrocytes in PSP (11), GFA was predominant in the putamen of ARTAG in AD, whereas tufted astrocytes were not.

This study revealed that the features associated with the presence of ARTAG differed between AD and PART. Two factors, age at death and NFT Braak stage, were consistently significant across each subtype of ARTAG in PART, while heterogeneous factors such as aging, sex, and Thal phase related to the generation of different subtypes of ARTAG in AD. Interestingly, male gender was found to influence the ARTAG formation in AD, which is consistent with previous findings (3). A study by Arena et al recently assessed the detailed immunophenotypic characteristics of chronic traumatic encephalopathy (CTE) in 14 cases (13). They revealed that astroglial tau pathology in CTE consisted of 4-repeat tau-positive astrogliopathy, which is indistinguishable from the TSA of ARTAG. The association between CTE and sex difference has not been well investigated because female professionals that are involved in contact sports are generally younger and not enough female brains with a history of repetitive head impacts have been donated for study on a regular basis (14). This said, almost all pathologically proven CTE patients have been male while only one patient was female. Therefore, there may be a common underlying pathological mechanism behind these two tauopathies (14, 15).

Our results also demonstrated that white matter ARTAG was associated with the Thal phase, which is also consistent with a previous report (3). Astrocytes surrounding senile plaques manifest a hypertrophic state and rich GFAP expression (16, 17), and Aβ oligomers themselves provoke astrocyte dysfunction of synaptogenic and synaptic protective capacity (18, 19). White matter ARTAG might be affected by neocortical impairment due to senile plaques because tau aggregation in white matter astroglia is distributed along axonal fibers.

The aging and Braak stages were extensively significant for ARTAG formation in the PART. Senescent astrocytes profoundly modify the cerebral microenvironment by increasing GFAP, vimentin, and senescence-associated secretory phenotype factors (20–22). A recent report revealed that insoluble tau species were less toxic to neurons and astrocytes than soluble species; and neural tau transfer to astrocytes prompted astrocytic tau aggregation (23, 24). Moreover, astrocytes physiologically express very low levels of tau. Therefore, they may relate to cerebral environmental alteration of neural tau increment, and aggregated tau in astrocytes of PART might indicate a slow collapse of aging brain homeostasis (23, 25–27). In contrast, however, several heterogeneous factors were associated with the existence of ARTAG in AD, and the pathological mechanisms influenced by tau pathology might include more elements besides Aβ toxicity, blood-brain barrier dysfunction, and chronic inflammation. On the other hand, the results of logistic regression analysis at the entire population level differed from that of previous investigations (3, 4). Discrepancies among the factors associated with ARTAG can be observed between our study and the previous investigations (3, 4), as well as between the foregoing studies (3, 4). This result may be due to the differences in population samples, which suggests that ARTAG formation can be associated with heterogeneous pathological conditions.

To our knowledge, this is the first study to evaluate astroglial tauopathy of the olfactory nerve. Astrocytic tau aggregation of the olfactory nerve was predominantly composed of subpial injuries. Astroglial tauopathies of the olfactory nerve tract were observed in close proximity to subpial tau aggregation in severe cases, where tau astrogliopathy was absent in the anterior olfactory nuclei despite an abundance of NFT and NT. Almost all astrocytic phosphorylated-tau components were 4-repeat tau in immunohistochemical studies, and confocal double

immunofluorescence staining revealed colocalization of phosphorylated-tau and GFAP. These results were consistent with previous research on ARTAG. As such, we assessed the tau astrogliopathies of the olfactory nerve encompassed within ARTAG (1, 3). The olfactory nerve is particular vulnerable to numerous neurodegenerative diseases, such as AD and Parkinson disease (28, 29). Since olfactory dysfunction is a prodromal symptom of various neurodegeneration and the olfactory epithelium is exposed to the external environment, the olfactory nerve could represent an entry site for pathogens (28, 30). The ARTAG of the olfactory nerve was milder than that of the amygdala, and these tau aggregations tended to be distributed over the proximal part of the olfactory nerve. It is well-established that Lewy body pathology propagates from the peripheral olfactory nerve to the CNS, while ARTAG might initiate from the amygdala and subsequently spread to the olfactory nerve (31, 32). In our study, ARTAG was absent in the anterior olfactory nucleus despite the abundance of NFT. Astrocytes have diverse functions and do not contribute to the brain microenvironment consistently (33, 34). Astrocytes play multiple roles in maintaining homeostasis in respective brain areas, which might play a role in the vulnerability of individual cerebral areas. The divergent distribution of ARTAG might be a reflection of various astrocyte reactions to aging alternation and tau toxicity between distinct brain regions.

Many matters remain to be assessed regarding the relationship between ARTAG and clinical aspects. Some previous studies showed that the ARTAG frequency of atypical AD was equal to that of typical AD, or no clinical impact was observed regarding ARTAG (3, 35). Other investigators reported that the densities of subcortical white matter TSAs in AD were associated with language and spatial dysfunction, or that AD cases who were diagnosed with possible progressive primary aphasia frequently contained cortical/subcortical TSA (12, 36). We

categorized patients with AD based on the presence of subcortical white matter ARTAG and compared their total MMSE scores related to language function. White matter ARTAG-positive AD tended to score lower with regard to language function despite having similar total MMSE scores, which is consistent with a previous report (12). Since we had to use brief neuropsychological examinations such as MMSE, we could not detect significant difference between the two. Astrocytes play important roles in myelin homeostasis by secreting regenerative factors, cholesterol metabolism, and myelin turnover (37–40). Disturbances in astrocytes as a result of tau toxicity may impede salient connections required for language.

A reduction in the number and morphological changes of astrocytes in patients with major depressive disorder has previously been reported (41, 42). These investigations suggest that astrocytes play an important role in neuropsychiatric disorders. Our retrospective review of medical records failed to reveal a significant relationship between ARTAG and mood/psychotic symptoms. Systematic quantitative scrutiny of mood/psychotic dysfunction was not part of the Hisayama study, and this research relied on daily medical records. Therefore, further research is needed to elucidate the effect of ARTAG on psychological disorders.

There are certain limitations of this study. Some cases with a severe burden of tauopathy were problematic in assessing whether lesions originated from neurons or glial cells. Our examination included only obvious astrocytic tauopathy. Therefore, this study may have underestimated the burden of ARTAG. We assessed only 5 brain sites of subependymal lesions as all the specimens did not include vicinities of the cerebral ventricle. Therefore, the analysis of ARTAG around the lateral ventricle and third ventricle was insufficient. This research is based on autopsy examinations in a Japanese population sample. Although autopsy rate in the sample was high, not

every deceased patient was examined. Thus, we cannot exclude a selection bias. In addition, different lifestyles and genetic backgrounds may limit the generalizability of our findings to other (in particular, Western) ethnicities. It was also difficult to perform neuropsychological tests at the terminal phase of dementia, and MMSE data were acquired at the early time of dementia onset. Furthermore, it was difficult to verify the presence of ARTAG is associated with cognitive impairment.

In conclusion, we investigated ARTAG in residents of a Japanese community. The amygdala represents a common hotspot of ARTAG in 2 alternative states of senescence, PART without dementia and AD. However, gray matter ARTAG was prominent in the putamen and middle frontal gyrus in AD following glial tauopathy in the amygdala. A multiple logistic regression analysis revealed that age at death and NFT Braak staging had a significant effect on the existence of ARTAG in HC, while male sex was found to have a significant effect on gray/white matter ARTAG. Moreover, the Thal phase significantly affected white matter ARTAG in AD. These results demonstrated the heterogeneous and complex pathomechanisms that were associated with ARTAG formation in the context of AD and HC.

ACKNOWLEDGMENTS

The authors thank the members of the Hisayama Research Institute for Lifestyle Diseases for their technical assistance. We would like to thank Editage (www.editage.com) for English language editing.

REFERENCES

1. Kovacs GG, Ferrer I, Grinberg LT, et al. Aging-related tau astrogliopathy (ARTAG): harmonized evaluation strategy. Acta Neuropathol 2016;131:87–102
2. Ikeda K, Akiyama H, Arai T, et al. Glial tau pathology in neurodegenerative diseases: Their nature and comparison with neuronal tangles. Neurobiol Aging 1998;19:S85-S91
3. Kovacs GG, Robinson JL, Xie SX, et al. Evaluating the patterns of aging-related tau astrogliopathy unravels novel insights into brain aging and neurodegenerative diseases. J Neuropathol Exp Neurol 2017;76:270–88
4. Miki T, Yokota O, Haraguchi T, et al. Factors associated with development and distribution of granular/fuzzy astrocytes in neurodegenerative diseases. Brain Pathol 2020;30:811–30
5. Kovacs GG, Xie SX, Robinson JL, et al. Sequential stages and distribution patterns of aging-related tau astrogliopathy (ARTAG) in the human brain. Acta Neuropathol Commun 2018;6:50
6. Honda H, Sasaki K, Hamasaki H, et al. Trends in autopsy-verified dementia prevalence over 29 years of the Hisayama study Neuropathology 2016;36:383–7
7. Hamasaki H, Honda H, Okamoto T, et al. Recent Increases in Hippocampal Tau Pathology in the Aging Japanese Population: The Hisayama Study. J Alzheimers Dis 2017;55:613–24
8. Matsuzaki T, Sasaki K, Tanizaki Y, et al. Insulin resistance is associated with the pathology of Alzheimer disease: the Hisayama study. Neurology 2010;75:764–70
9. Kubo M, Hata J, Doi Y, et al. Secular Trends in the Incidence of and Risk Factors for Ischemic Stroke and Its Subtypes in Japanese Population. Circulation 2008;118:2672–8
10. Izumaru K, Hata J, Nakano T, et al. Reduced Estimated GFR and Cardiac Remodeling: A

Population-Based Autopsy Study. Am J Kidney Dis 2019;74:373–81

11. Kovacs GG, Lukic MJ, Irwin DJ, et al. Distribution patterns of tau pathology in progressive supranuclear palsy. Acta Neuropathol 2020;140:99–119

12. Resende EDPF, Nolan AL, Petersen C, et al. Language and spatial dysfunction in Alzheimer disease with white matter thorn-shaped astrocytes. Neurology 2020;94:E1353–64

13. Arena JD, Smith DH, Lee EB, et al. Tau immunophenotypes in chronic traumatic encephalopathy recapitulate those of ageing and Alzheimer's disease. Brain 2020;143:1572–87

14. Phelps A, Mez J, Stern RA, et al. Risk factors for chronic traumatic encephalopathy: A proposed framework. Semin Neurol 2020;40:439–49

15. Roberts GW, Whitwell HL, Acland PR, et al. Dementia in a punch-drunk wife. Lancet 1990;335:918–9

16. Heneka MT, Carson MJ, Khoury J El, et al. Neuroinflammation in Alzheimer's disease. Lancet Neurology 2015;14:388-405

17. Olabarria M, Noristani HN, Verkhratsky A, et al. Concomitant astroglial atrophy and astrogliosis in a triple transgenic animal model of Alzheimer's disease. Glia 2010;58:831–8

18. Diniz LP, Tortelli V, Matias I, et al. Astrocyte transforming growth factor beta 1 protects synapses against Aβ oligomers in Alzheimer's disease model. J Neurosci 2017;37:6797–809

19. Matias I, Morgado J, Gomes FCA. Astrocyte Heterogeneity: Impact to Brain Aging and Disease. Front Aging Neurosci 2019;11:59

20. Clarke LE, Liddelow SA, Chakraborty C, et al. Normal aging induces A1-like astrocyte

reactivity. Proc Natl Acad Sci U S A 2018;115:E1896–905

21. Mombach JCM, Vendrusculo B, Bugs CA. A model for p38MAPK-induced astrocyte senescence. PLoS One 2015;10: e0125217

22. Porchet R, Probst A, Bouras C, et al. Analysis of gial acidic fibrillary protein in the human entorhinal cortex during aging and in Alzheimer's disease. Proteomics 2003;3:1476-85

23. Maté De Gérando A, D'Orange M, Augustin E, et al. Neuronal tau species transfer to astrocytes and induce their loss according to tau aggregation state. Brain 2021;144:1167–82

24. D'Orange M, Aurégan G, Cheramy D, et al. Potentiating tangle formation reduces acute toxicity of soluble tau species in the rat. Brain 2018;141:535–49

25. Asai H, Ikezu S, Tsunoda S, et al. Depletion of microglia and inhibition of exosome synthesis halt tau propagation. Nat Neurosci 2015;18:1584–93

26. Kahlson MA, Colodner KJ. Glial tau pathology in tauopathies: Functional consequences. J Exp Neurosci 2016 PMID: 26884683

27. Chiarini A, Armato U, Gardenal E, et al. Amyloid β-exposed human astrocytes overproduce phospho-tau and overrelease it within exosomes, effects suppressed by calcilytic NPS 2143-Further implications for Alzheimer's therapy. Front Neurosci 2017;11:217

28. Rey NL, Wesson DW, Brundin P. The olfactory bulb as the entry site for prion-like propagation in neurodegenerative diseases. Neurobiol Dis 2018;109:226–48

29. Ubeda-Bañon I, Saiz-Sanchez D, Flores-Cuadrado A, et al. The human olfactory system in two proteinopathies: Alzheimer's and Parkinson's diseases. Transl Neurodegener. 2020;9:22

30. Dando SJ, Mackay-Sim A, Norton R, et al. Pathogens penetrating the central nervous system: Infection pathways and the cellular and molecular mechanisms of invasion. Clin

Microbiol Rev 2014;27:691–726

31. Braak H, Ghebremedhin E, Rüb U,et al. Stages in the development of Parkinson's disease-related pathology. Cell Tissue Res 2004;318:121-34

32. Braak H, Del Tredici K, Rüb U, et al. Staging of brain pathology related to sporadic Parkinson's disease. Neurobiol Aging 2003;24:197–211

33. Chai H, Diaz-Castro B, Shigetomi E, et al. Neural Circuit-Specialized Astrocytes: Transcriptomic, Proteomic, Morphological, and Functional Evidence. Neuron 2017;95:531-549.

34. Rasmussen R, Samson AJ. Astrocytes: Tailored to Support the Demand of Neural Circuits? Cell Syst 2017;5:165-7

35. Nolan A, De Paula Franca Resende E, Petersen C, et al. Astrocytic tau deposition is frequent in typical and atypical Alzheimer disease presentations. J Neuropathol Exp Neurol 2019;78:1112–23

36. Munoz DG, Woulfe J, Kertesz A. Argyrophilic thorny astrocyte clusters in association with Alzheimer's disease pathology in possible primary progressive aphasia. Acta Neuropathol 2007;114:347–57

37. Berghoff SA, Gerndt N, Winchenbach J, et al. Dietary cholesterol promotes repair of demyelinated lesions in the adult brain. Nat Commun 2017;8:1–15

38. Albrecht PJ, Murtie JC, Ness JK, et al. Astrocytes produce CNTF during the remyelination phase of viral-induced spinal cord demyelination to stimulate FGF-2 production. Neurobiol Dis 2003;13:89–101

39. Dutta DJ, Woo DH, Lee PR, et al. Regulation of myelin structure and conduction velocity by perinodal astrocytes. Proc Natl Acad Sci U S A 2018;115:11832–7

40. Varela-Echevarría A, Vargas-Barroso V, Lozano-Flores C, et al. Is there evidence for

myelin modeling by astrocytes in the normal adult brain? Front Neuroanat 2017;11:75

41. Rajkowska G, Hughes J, Stockmeier CA, et al. Coverage of blood vessels by astrocytic endfeet is reduced in major depressive disorder. Biol Psychiatry 2013;73:613–21

42. Cotter D, Mackay D, Chana G, et al. Reduced neuronal size and glial cell density in area 9 of the dorsolateral prefrontal cortex in subjects with major depressive disorder. Cereb Cortex 2002;12:386–94

Figure legends

Figure 1. Representative histology of ARTAG. (**A-C**) Subependymal and perivascular ARTAG in the amygdala of a cognitive healthy PART subject. Immunohistochemical analysis of phosphorylated tau (AT8) revealed thorn-shaped astrocytes (TSA) with dense tau deposits in subependymal (**B**) and perivascular areas (**C**). (**D-F**) Amygdala of the same case also exhibited gray matter and white matter ARTAG. Gray matter ARTAG mostly consisted of granular/fuzzy astrocytes (**E**) while most of white matter ARTAG consisted of TSA (**F**). Representative subpial ARTAG in a subject with Alzheimer disease demonstrated their phosphorylated tau components (**G**: AT8), which comprised 4-repeat tau (**I**: RD4), but not 3-repeat tau (**H**: RD3).

Figure 2. Mosaic plot of each ARTAG distribution subtype with respect to Alzheimer disease (AD) and cognitively healthy cases (HC). Asterisks denotes the sites exhibiting mild ARTAG with significant difference to that of amygdala by Steel-Dwass test ($p < 0.05$). MFG, middle frontal gyrus; STG/MTG, superior temporal gyrus and middle temporal gyrus; PVC, primary visual cortex; Hippo, hippocampus; Parahippo, parahippocampal gyrus; Amyg, amygdala; OlfN, olfactory nerve; Put, putamen; GP, globus pallidus; MB, midbrain; MO, medulla oblongata.

Figure 3. Representative images of astroglial tauopathy of olfactory nerves. A-C: Immunohistochemical study of phosphorylated tau (AT8) revealed thorn-shaped astrocytes (TSA) in subpial regions of olfactory nerves (**A, B**); fewer white matter TSA were observed in the vicinity (**A, C**). (**D-F**) Anterior olfactory nucleus frequently manifested neurofibrillary tangles; however, no obvious glial tauopathy was observed. **G-I**: The tau astrogliopathy of olfactory nerves is composed of 4-repeat tau (**I**: RD4), but not 3-repeat tau (**H**: RD3), similar to ARTAG in other brain sites. (**J-L**) Confocal images of the subpial region of the olfactory nerve

demonstrate that most of the AT8-positive structures (represented in red) were localized in association with the GFAP-positive cellular components (represented in green).

Figure. 1

Click here to access/download;Figure;fiugre1.tif

Ł†…ª äª ª ª ª ª ‹ª⁄ª⁄ª …

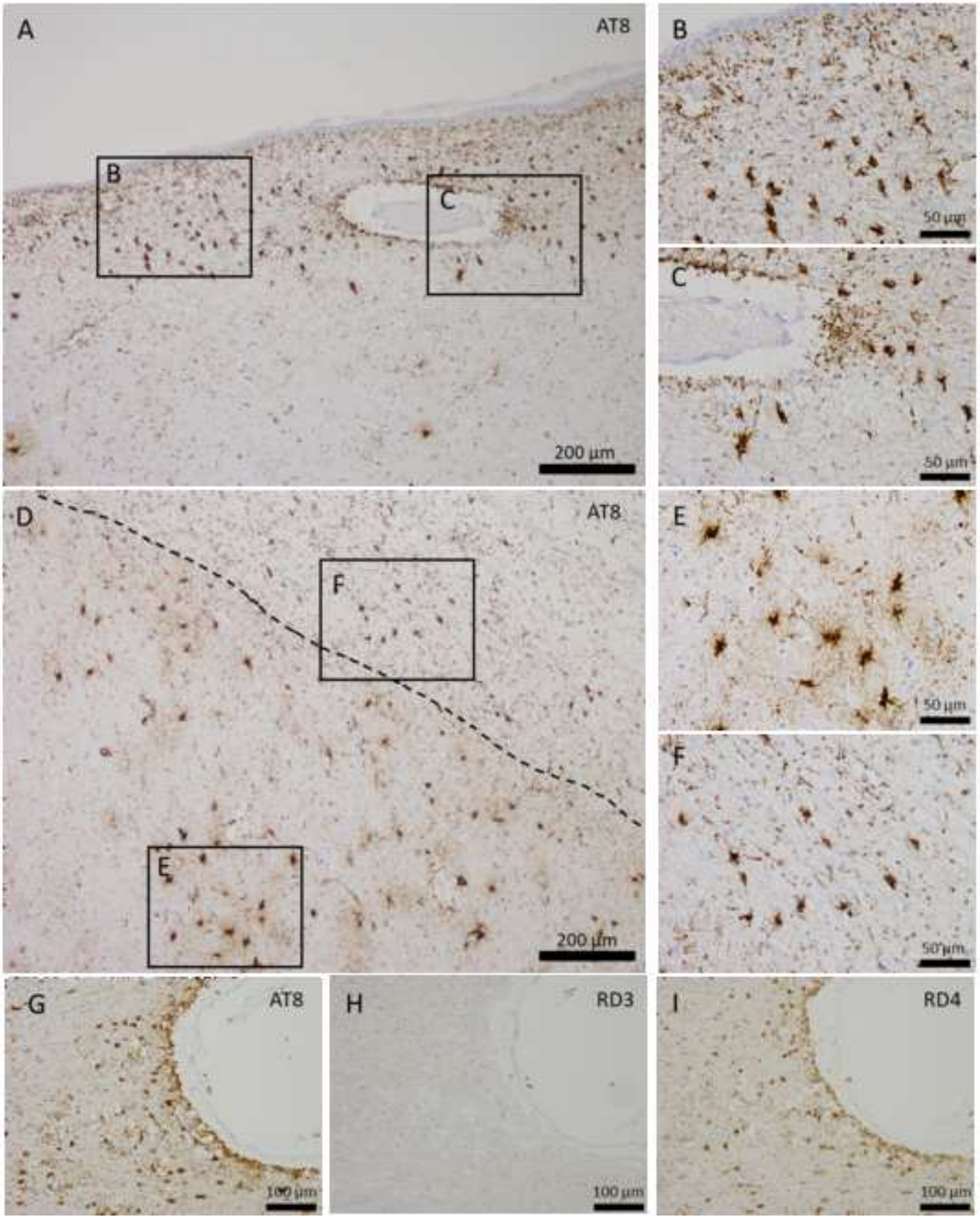

Figure. 2

Click here to access/download;Figure;figure2.tif

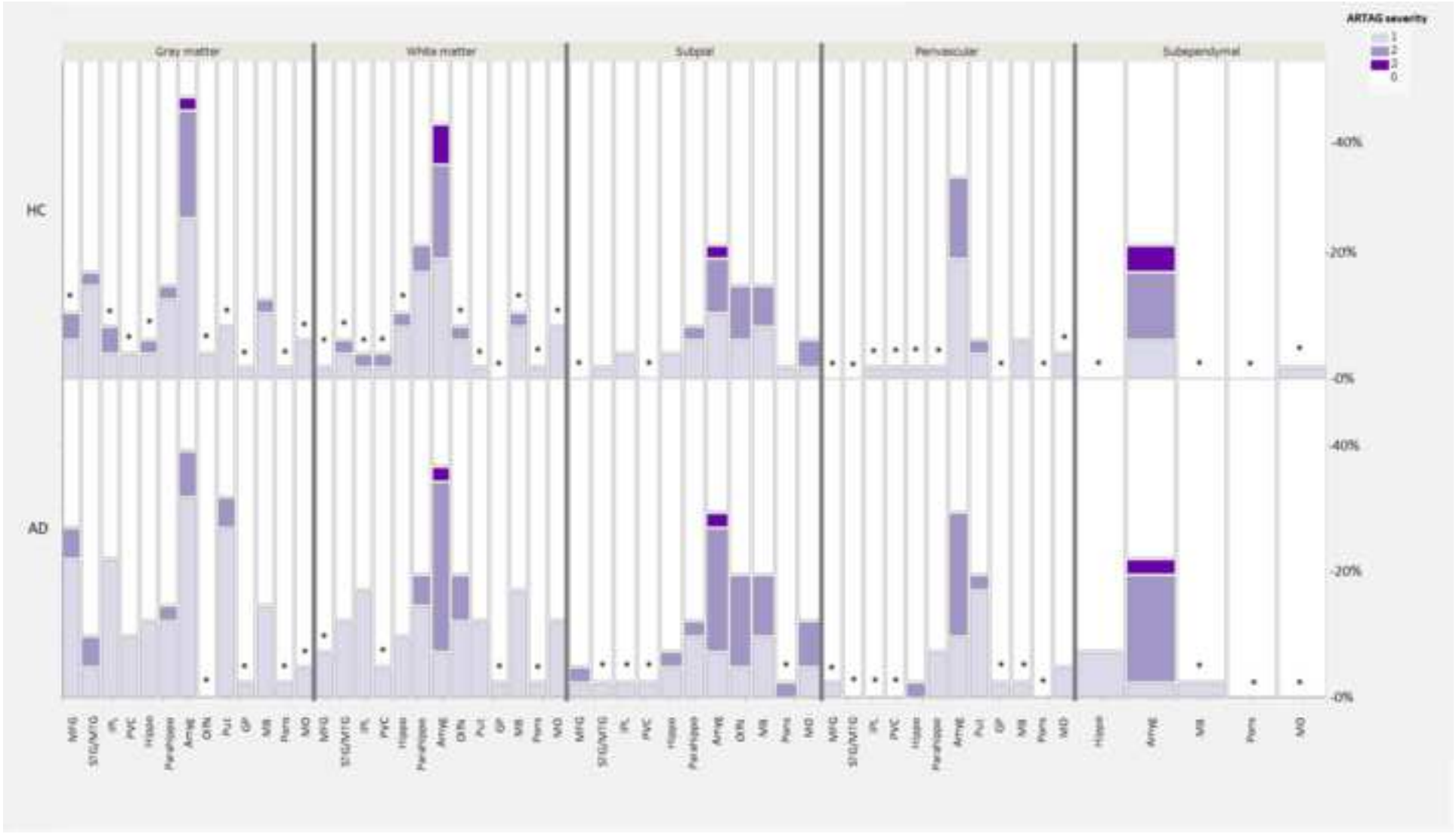

Figure. 3

Click here to access/download;Figure;figure3.tif

Ł†…ª ä› ª ª ª ª ª ‹ª⁄ª⁄ª …

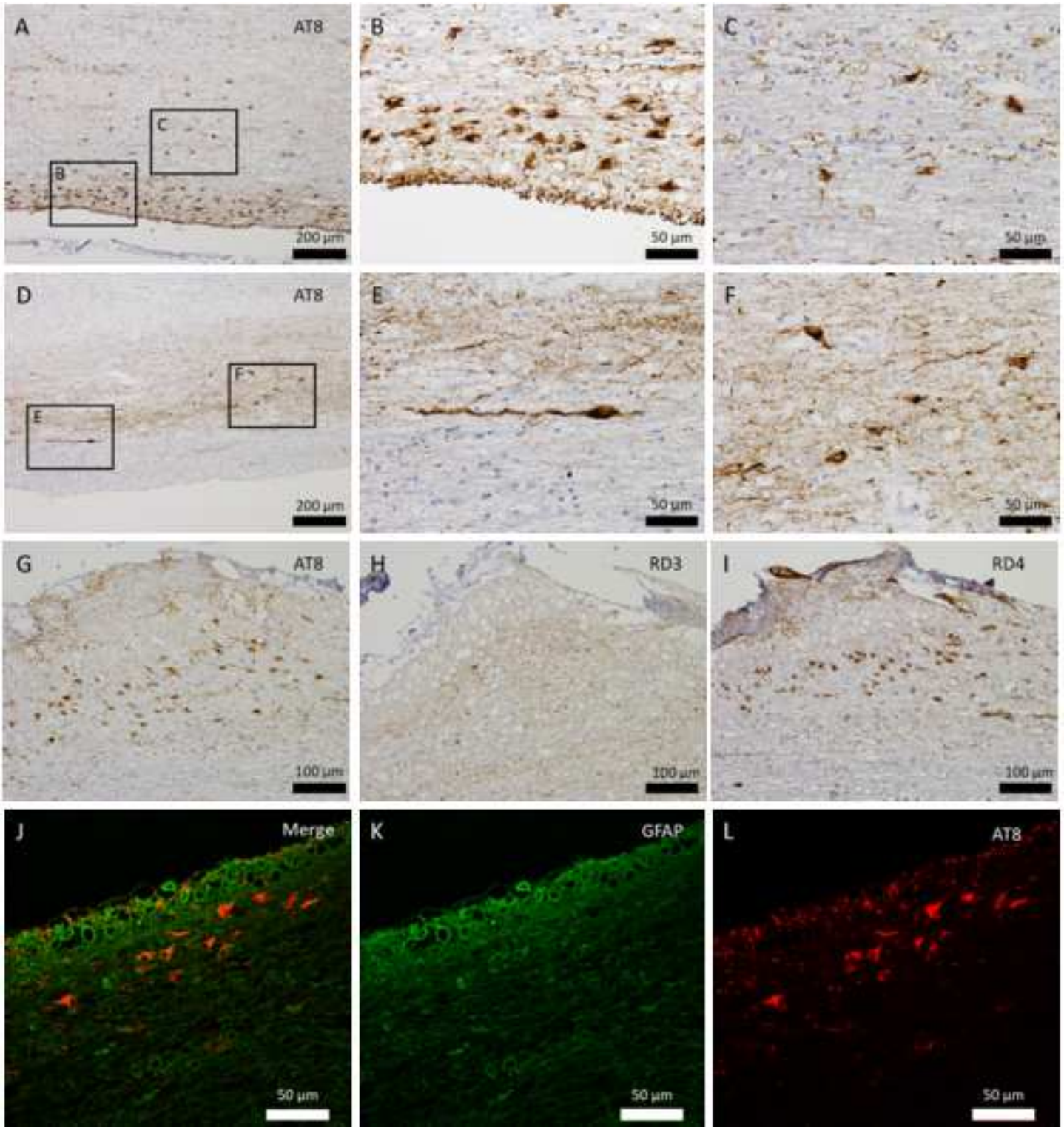

Table

Table 1. Summary of All Examined Cases and Frequency of ARTAG

Clinicopathological Diagnosis	Number	Female	Mean Age at Death (±SD)	Brain Weight (±SD)	NFT Braak (mean)	Thal Phase (mean)	CERAD (mean)	AT ARTAG (%)	SP ARTAG (%)	SE ARTAG (%)	GM ARTAG (%)	WM ARTAG (%)	PV ARTAG (%)
HC	47	13 (27.7%)	80.7 (±9.83)	1250 (±114.1)	3.38	1.1	0.9	53	26	21	51	43	34
AD	41	25 (60.1%)	90.1 (±6.03)	1156 (±116.1)	5.20	4.4	3.0	80	56	29	68	56	39
VD	8	2 (25%)	85.8 (±7.30)	1238 (±165.1)	3.75	1.6	1.4	100	88	38	75	88	63
DLB	5	1 (20%)	83.0 (±5.24)	1358 (±153.9)	4.60	1.6	1.6	40	40	20	20	20	20
PSP	3	1 (33.3%)	82.3 (±6.66)	1157 (±210.1)	5.00	0.6	1.0	100	100	100	100	100	67
AGD	2	1 (50%)	88.0 (±1.41)	975 (±247.5)	4.00	1.5	1.0	100	100	0	100	100	0
SD-NFT	4	3 (75%)	93.3 (±11.95)	1120 (±191.3)	5.00	0.8	1.3	100	75	100	100	100	75

Abbreviations: HC, cognitive healthy case; AD, Alzheimer disease; VD, vascular dementia; DLB, dementia with Lewy body; PSP, progressive supranuclear palsy; AGD, argyrophilic grain dementia; SD-NFT, senile dementia of the neurofibrillary tangle type; AT, all type; SP, subpial; SE, subependymal; GM, gray matter; WM, white matter; PV, perivascular.

Table

Table 2. Logistic Regression Models of the Effect of Clinical and Pathological Variables on the Presence of ARTAG in All Cases

		Univariate Logistic Regression Models			Multiple Logistic Regression Models		
		OR	95% CI	p value	OR	95% CI	p value
All type	Age at death	**1.06**	(1.05, 1.07)	**<.0001**	**1.06**	(1.05, 1.08)	**<.0001**
	Sex (Male)	1.03	(0.87, 1.21)	0.75	**1.63**	(1.36, 1.95)	**<.0001**
	Thal phase	1.00	(0.96, 1.05)	0.84	**0.85**	(0.81, 0.89)	**<.0001**
	NFT Braak stage	**1.52**	(1.40, 1.64)	**<.0001**	**1.53**	(1.39, 1.68)	**<.0001**
Subpial	Age at death	**1.08**	(1.05, 1.10)	**<.0001**	**1.08**	(1.05, 1.11)	**<.0001**
	Sex (Male)	0.87	(0.59, 1.27)	0.46	1.50	(0.99, 2.27)	0.058
	Thal phase	1.03	(0.94, 1.14)	0.49	**0.87**	(0.78, 0.97)	**0.011**
	NFT Braak stage	**1.50**	(1.26, 1.80)	**<.0001**	**1.43**	(1.15, 1.78)	**0.0013**
Subependymal	Age at death	**1.06**	(1.02, 1.10)	**0.0067**	**1.06**	(1.01, 1.11)	**0.012**
	Sex (Male)	0.97	(0.51, 1.86)	0.93	1.48	(0.73, 3.02)	0.28
	Thal phase	0.96	(0.82, 1.13)	0.62	**0.80**	(0.67, 0.97)	**0.021**
	NFT Braak stage	**1.53**	(1.11, 2.09)	**0.0085**	**1.62**	(1.10, 2.39)	**0.016**
Gray matter	Age at death	**1.04**	(1.03, 1.06)	**<.0001**	**1.05**	(1.03, 1.07)	**<.0001**
	Sex (Male)	1.26	(0.93, 1.70)	0.13	**1.91**	(1.37, 2.66)	**0.0001**
	Thal phase	0.99	(0.92, 1.06)	0.73	**0.84**	(0.77, 0.92)	**<.0001**
	NFT Braak stage	**1.53**	(1.33, 1.76)	**<.0001**	**1.60**	(1.36, 1.90)	**<.0001**
White matter	Age at death	**1.06**	(1.04, 1.08)	**<.0001**	**1.07**	(1.04, 1.09)	**<.0001**
	Sex (Male)	1.04	(0.77, 1.41)	0.80	**1.67**	(1.19, 2.34)	**0.0029**
	Thal phase	0.99	(0.92, 1.07)	0.80	**0.83**	(0.76, 0.90)	**<.0001**
	NFT Braak stage	**1.56**	(1.36, 1.81)	**<.0001**	**1.61**	(1.35, 1.93)	**<.0001**
Perivascular	Age at death	**1.07**	(1.04, 1.11)	**<.0001**	**1.08**	(1.04, 1.11)	**<.0001**
	Sex (Male)	0.81	(0.51, 1.28)	0.37	1.35	(0.82, 2.22)	0.24
	Thal phase	1.06	(0.95, 1.19)	0.31	0.91	(0.78, 1.04)	0.15
	NFT Braak stage	**1.47**	(1.18, 1.83)	**0.0006**	**1.35**	(1.04, 1.76)	**0.023**

Table

Table 3. Logistic Regression Models of the Effects of Clinical and Pathological Variables on the Presence of ARTAG in AD Cases

		Univariate Logistic Regression Models				Multiple Logistic Regression Models			
		OR	95% CI		p value	OR	95% CI		p value
All type	Age at Death	**1.05**	(1.02,	1.07)	**<0.0001**	**1.06**	(1.04,	1.09)	**<0.0001**
	Sex (Male)	**2.00**	(1.52,	2.62)	**<0.0001**	**2.16**	(1.63,	2.87)	**<0.0001**
	Thal Phase	1.17	(0.99,	1.38)	0.053	**1.33**	(1.11,	1.60)	**0.0013**
	NFT Braak Stage	0.98	(0.77,	1.25)	0.86	0.75	(0.58,	0.98)	**0.035**
Subpial	Age at Death	**1.07**	(1.02,	1.13)	**0.0073**	**1.08**	(1.03,	1.15)	**0.0028**
	Sex (Male)	1.73	(0.94,	3.17)	0.077	1.74	(0.92,	3.30)	0.09
	Thal Phase	1.16	(0.8,	1.68)	0.42	1.29	(0.86,	1.93)	0.21
	NFT Braak Stage	1.24	(0.72,	2.16)	0.43	1.04	(0.56,	1.91)	0.91
Subependymal	Age at Death	1.05	(0.96,	1.15)	0.31	1.004	(0.95,	1.16)	0.35
	Sex (Male)	1.90	(0.62,	5.88)	0.26	1.60	(0.49,	5.23)	0.44
	Thal Phase	0.96	(0.52,	1.79)	0.9	0.84	(0.42,	1.71)	0.64
	NFT Braak Stage	1.95	(0.7,	5.46)	0.2	2.13	(0.62,	7.35)	0.22
Gray matter	Age at Death	**1.05**	(1.01,	1.09)	**0.027**	**1.06**	(1.02,	1.12)	**0.0066**
	Sex (Male)	**2.30**	(1.41,	3.74)	**0.0008**	**2.67**	(1.60,	4.44)	**0.0001**
	Thal Phase	1.10	(0.83,	1.46)	0.51	1.31	(0.95,	1.80)	0.086
	NFT Braak Stage	0.77	(0.5,	1.20)	0.24	**0.58**	(0.36,	0.93)	**0.024**
White matter	Age at Death	**1.04**	(1.00,	1.09)	**0.048**	**1.06**	(1.02,	1.11)	**0.006**
	Sex (Male)	**2.11**	(1.28,	3.50)	**0.0036**	**2.51**	(1.47,	4.27)	**0.0006**
	Thal Phase	1.32	(0.95,	1.82)	0.082	**1.64**	(1.15,	2.35)	**0.0038**
	NFT Braak Stage	0.73	(0.46,	1.15)	0.17	**0.50**	(0.31,	0.82)	**0.0055**
Perivascular	Age at Death	1.03	(0.97,	1.10)	0.37	1.03	(0.97,	1.11)	0.28
	Sex (Male)	1.73	(0.82,	3.67)	0.15	1.58	(0.73,	3.43)	0.25
	Thal Phase	1.23	(0.76,	1.99)	0.37	1.15	(0.69,	1.92)	0.6
	NFT Braak Stage	1.69	(0.85,	3.34)	0.13	1.46	(0.68,	3.13)	0.33

Table

Table 4. ~~Logistic regression models~~ Logistic Regression Models of the Effects of Clinical and Pathological Variables on the Presence of ARTAG in HC

Cases~~regarding effect of variables on the presence of ARTAG in HC~~

Formatted: Normal, Indent: Left: 0", First line: 0.5", Space Before: 0 pt

Formatted: Normal, Indent: First line: 0.5"

		Univariate Logistic Regression Models				Multiple Logistic Regression Models			
		OR	95% CI		p value	OR	95% CI		p value
All type	Age at Death	1.1	(1.08,	1.12)	**<0.0001**	1.1	(1.06,	1.11)	**<0.0001**
	Sex (Male)	0.59	(0.44,	0.8)	**0.0008**	1.2	(0.8,	1.68)	0.42
	Thal Phase	1.2	(1.06,	1.29)	**0.0027**	1.1	(0.98,	1.22)	0.1
	NFT Braak Stage	2.4	(2.03,	2.8)	**<0.0001**	2.2	(1.79,	2.57)	**<0.0001**
Subpial	Age at Death	1.1	(1.06,	1.15)	**<0.0001**	1.1	(1.02,	1.13)	**0.0058**
	Sex (Male)	0.47	(0.24,	0.93)	**0.035**	0.78	(0.34,	1.79)	0.57
	Thal Phase	1.1	(0.878,	1.40)	0.39	1.0	(0.79,	1.38)	0.76
	NFT Braak Stage	2.8	(1.87,	4.26)	**<0.0001**	2.7	(1.68,	4.33)	**<0.0001**
Subependymal	Age at Death	1.1	(1,	1.15)	**0.043**	1.0	(0.95,	1.13)	0.46
	Sex (Male)	0.66	(0.19,	2.32)	0.52	0.98	(0.23,	4.11)	0.97
	Thal Phase	1.3	(0.89,	1.94)	0.19	1.3	(0.86,	2.04)	0.22
	NFT Braak Stage	2.3	(1.18,	4.48)	**0.0046**	2.3	(1.06,	5.13)	**0.016**
Gray matter	Age at Death	1.1	(1.06,	1.13)	**<0.0001**	1.1	(1.05,	1.14)	**<0.0001**
	Sex (Male)	0.70	(0.41,	1.20)	0.2	1.5	(0.75,	2.84)	0.26
	Thal Phase	1.2	(0.97,	1.37)	0.12	1.1	(0.89,	1.30)	0.48
	NFT Braak Stage	2.1	(1.64,	2.77)	**<0.0001**	1.8	(1.36,	2.46)	**<0.0001**
White matter	Age at Death	1.1	(1.07,	1.15)	**<0.0001**	1.1	(1.05,	1.16)	**<0.0001**
	Sex (Male)	0.68	(0.38,	1.21)	0.2	1.5	(0.73,	3.21)	0.24
	Thal Phase	1.1	(0.94,	1.38)	0.18	1.1	(0.87,	1.32)	0.53
	NFT Braak Stage	2.7	(1.95,	3.71)	**<0.0001**	2.4	(1.67,	3.53)	**<0.0001**
Perivascular	Age at Death	1.1	(1.06,	1.17)	**<0.0001**	1.1	(1.02,	1.16)	**0.0056**
	Sex (Male)	0.39	(0.18,	0.85)	**0.02**	0.80	(0.31,	2.05)	0.64
	Thal Phase	1.3	(1.00,	1.66)	0.056	1.2	(0.91,	1.59)	0.21
	NFT Braak Stage	2.2	(1.46,	3.37)	**<0.0001**	2.1	(1.26,	3.43)	**0.0012**

Supplemental Figure. 1 (.tif)

Supplemental Table. 1 (.doc)

Supplemental Table. 2 (.doc)

Supplemental Table. 3 (.doc)

Supplemental Table. 4 (.doc)

Supplemental Table. 5 (.doc)